HHS Public Access

Author manuscript

Nat Rev Cancer. Author manuscript; available in PMC 2024 January 01.

Published in final edited form as:

Nat Rev Cancer. 2023 January ; 23(1): 25–42. doi:10.1038/s41568-022-00527-5.

Intravital imaging to study cancer progression and metastasis

David Entenberg[1,2,3], **Maja H. Oktay**[1,2,3,4], **John S. Condeelis**[1,2,4,5]

[1]Gruss Lipper Biophotonics Center, Albert Einstein College of Medicine/Montefiore Medical Center, Bronx, NY, USA.

[2]Integrated Imaging Program, Albert Einstein College of Medicine/Montefiore Medical Center, Bronx, NY, USA.

[3]Department of Pathology, Albert Einstein College of Medicine/Montefiore Medical Center, Bronx, NY, USA.

[4]Department of Surgery, Albert Einstein College of Medicine/Montefiore Medical Center, Bronx, NY, USA.

[5]Department of Cell Biology, Albert Einstein College of Medicine/Montefiore Medical Center, Bronx, NY, USA.

Abstract

Navigation through the bulk tumour, entry into the blood vasculature, survival in the circulation, exit at distant sites and resumption of proliferation are all steps necessary for tumour cells to successfully metastasize. The ability of tumour cells to complete these steps is highly dependent on the timing and sequence of the interactions that these cells have with the tumour microenvironment (TME), including stromal cells, the extracellular matrix and soluble factors. The TME thus plays a major role in determining the overall metastatic phenotype of tumours. The complexity and cause-and-effect dynamics of the TME cannot currently be recapitulated in vitro or inferred from studies of fixed tissue, and are best studied in vivo, in real time and at single-cell resolution. Intravital imaging (IVI) offers these capabilities, and recent years have been a time of immense growth and innovation in the field. Here we review some of the recent advances in IVI of mammalian models of cancer and describe how IVI is being used to understand cancer progression and metastasis, and to develop novel treatments and therapies. We describe new techniques that allow access to a range of tissue and cancer types, novel fluorescent reporters and biosensors that allow fate mapping and the probing of functional and phenotypic states, and the clinical applications that have arisen from applying these techniques, reporters and biosensors to study cancer. We finish by presenting some of the challenges that remain in the field, how to address them and future perspectives.

Correspondence should be addressed to David Entenberg, Maja H. Oktay or John S. Condeelis. david.entenberg@einsteinmed.edu; maja.oktay@einsteinmed.edu; john.condeelis@einsteinmed.edu.

Author contributions

All authors researched data for the article, contributed substantially to discussion of the content, wrote the article, and reviewed and/or edited the manuscript before submission.

Competing interests

The authors declare no competing interests.

Introduction

Although most cancer deaths are due to metastasis[1], the mechanisms of primary and metastatic tumour progression continue to elude definitive resolution, despite many studies[2]. This makes the opening sentence of Warren and Gates's 1936 article as relevant today as when it was first published: "In spite of a large volume of information from clinical and experimental observations on tumour metastasis, the subject is still largely a matter of speculation"[3]. The ultimate result of this uncertainty is that many promising new drugs that target metastatic cancer fail during clinical trials owing to lack of therapeutic efficacy[4,5]. Furthermore, more than 10 years of investigation into the tumour microenvironment (TME) has revealed that the TME is a major driver of metastatic phenotypes[6,7]. A full understanding of the TME, in both primary and secondary sites, is therefore crucial to reveal commonalities and differences between these sites that could lead to successful treatments.

Since the TME encompasses host and tumour cells, the most 'high-fidelity' experimental method to study this biology would be in vivo studies in mammals that measure cells of the TME in real time, longitudinally (at multiple time points) and with single-cell resolution. Intravital imaging (IVI) is beginning to fill this role as it provides insights into the TMEs and cell phenotypes that drive the timing, location and aggressiveness of tumour cell growth, invasion, dissemination to distant sites and therapeutic response, all within intact live tissues.

Here we review some of the recent advances in IVI that make investigations into cancer progression and metastasis, and their treatment, possible. We begin by making the case for the necessity of investigating tumour cell phenotypes in vivo, and then discuss some of the advances that have enhanced the ease of use (via improved methods and protocols) and utility of IVI (by increasing the amount and type of information the technique can record).

We confine this Review to the imaging of mouse models of cancer, as these are currently the best models available for the investigation of human cancer. In addition, this Review is focused on IVI using multiphoton microscopy because multiphoton microscopy offers significant advantages over clinical techniques such as magnetic resonance imaging and positron emission tomography (for example, single-cell resolution and functional labelling[8,9]), as well as other types of optical microscopy, such as confocal microscopy (for example, reduced photobleaching, increased penetration depth, more robust optical alignment and increased sensitivity to weak fluorophores[10]). Furthermore, we describe the clinical impact that IVI-discovered phenotypes and pathways are having on the discovery of new biomarkers and therapeutics.

Advances in multiphoton IVI

Introduction to multiphoton IVI

The fundamentals of confocal and multiphoton microscopy[10,11], and of IVI and its history, have been described in many publications[12-18] that provide excellent explanations for how these imaging methods generate images of single slices of intact tissues. They describe how confocal microscopes achieve this by blocking out-of-focus light with pinholes before the detector, and how multiphoton microscopes limit the generated signal to the focal plane by

using ultrafast pulsed infrared laser sources that allow absorption to occur only at regions of the sample with the highest photon density (that is, the plane of focus). Confocal and multiphoton microscopes can non-destructively produce images of optical sections that are comparable to the mechanically sliced tissue sections of standard histopathology. Several excellent reviews have additionally been published covering applications of IVI, such as the use of fluorescent proteins for visualizing single[19-22] and multiple[23,24] cell types; the utility of implantable imaging windows[25,26]; the use of IVI for measuring metastasis[9,27], cell signalling[28], molecular dynamics[29] and stem cell plasticity[30] in vivo; the use of IVI in anticancer drug research[31]; and the use of IVI directly in the clinic[32].

Enhancing the accessibility of multiphoton IVI

Although IVI is typically considered a technically difficult process[33] requiring specialized equipment [27,34] and significant skills, the past decade has seen substantial growth of IVI use, and barriers to its adoption have been dramatically reduced. Advances (Box 1) include the advent of a plethora of new microscope technologies[35-38], fluorescent biosensors for identifying cell types and biochemical pathways[39-41], and protocols for accessing various tissues throughout the body, both short-term and long-term[25,26,32]. Of particular importance are the numerous surgical protocols for accessing and stabilizing tissues that have enabled extended time-lapse intravital multiphoton imaging in a variety of murine organs, including the brain[42], liver[43,44], cremaster muscle[45], spinal cord[46,47], mammary glands[48] and tumours[27,49], ovaries[50], kidneys[51], lymphatic vessels[52,53], lymph nodes[54,55], salivary glands[56], lungs[57,58], and even developing embryos[59]. The images presented in Fig. 1 are examples of the range and variety of tissues that can be imaged, and visually demonstrate how IVI has improved beyond the days of blurry black-and-white images to a level that is now comparable to that of in vitro or ex vivo studies.

Crucial to the success of these advances is the ability to prepare tissue for IVI. To achieve this, researchers are turning to surgical engineering, a field combining mechanical engineering, materials science and surgery that has traditionally focused on the unidirectional flow of engineering technology into the clinic (developing novel materials, devices and surgical protocols for use on patients)[60,61]. However, for IVI, this flow is reversed, and the skills of and the instruments and procedures used by surgeons are brought into the imaging laboratory. The influence of this process is particularly notable when it comes to the development of chronic, or implantable, imaging windows (Box 2). Material biocompatibility, mechanical design and surgical implantation protocols must all converge to create a portal into the underlying tissue that does not induce local or systemic inflammation, negatively impact the normal physiology or behaviour of the animal, or alter the biology being investigated (Box 3). Validation studies have shown that this goal is attainable[58,62,63]. Implantable imaging windows allow access to internal organs (even vital organs), while maintaining survival of the animal over days to weeks (or longer), enabling longitudinal IVI of tumour progression[58,62,63]. It is important to note that use of implantable imaging windows (Box 2) is extremely flexible and does not limit the application of any of the new microscope technologies described in Box 1.

With this enhanced accessibility, biologists can now use IVI to collect real-time in vivo information about the dynamic processes that cells and tissues undergo within their native TME in the live animal[58,64,65]. This ability even extends to measurements of the pharmacodynamics and pharmacokinetics of therapeutic treatments[66-68] and their influence on metastasis[69] (discussed further in the coming sections).

Expanding the spatial and temporal scale of imaging

TMEs have heterogeneous vascularization, extracellular matrix and cell density that may reflect distinct steps in cancer progression and need to be evaluated across different spatial scales (from submicron to the entire tumour). To record events on these vastly different scales, it is necessary to capture images of large volumes of the tumour tissue (~1–2 mm^3) at subcellular resolution (~0.25 μm per pixel)[48]. Unfortunately, capturing low-magnification images with high resolution is not possible with standard multiphoton microscopy, which relies on high-magnification, high numerical aperture objective lenses for efficient and bright signal generation[10]. This limits the size of the field of view of the acquired images and results in a dramatic undersampling of the tissues. The impact of this is illustrated in Fig. 2a, where just a few small regions from a picture of a famous person are presented. From just these small regions, it is impossible to discern the identity of the subject.

One solution is to acquire many high-magnification, high-resolution images of the subject in a contiguous mosaicked pattern (Fig. 2b), and then stitch them together to produce a low-magnification image that can reveal the underlying identity of the subject (Fig. 2c), a process called ‘large-volume, high-resolution’ (LVHR) imaging[70,71]. The application of LVHR to IVI (LVHR-IVI)[48] generates a more comprehensive view of the tumour than is possible with traditional IVI. Figure 2d demonstrates the type of images that can be obtained with LVHR-IVI techniques[48]. LVHR-IVI thus allows researchers to use IVI images in a manner similar to how pathologists use sections from formalin-fixed, paraffin-embedded tissue, where the extent of tumour invasion and regions of interest are first identified at low magnification and are then analysed in more detail at higher magnification. With use of tissue morphology, areas of stroma (regions devoid of endothelial or epithelial cells) and neo-angiogenic vasculature[72] can be identified. LVHR-IVI thus allows critical biological and pathological processes to be distinguished (for example, discerning mammary ductal carcinoma in situ (DCIS) from late carcinoma or branching ducts) following standard histopathology criteria[73]. More detailed analyses can then be performed at higher magnification, identifying growth patterns associated with tumour progression and dissemination (Fig. 2e-g).

Combining LVHR-IVI with imaging windows (Box 2) enables multiple imaging sessions spanning days to weeks, or even months. However, longitudinal imaging introduces the additional challenge of locating the same imaging field repeatedly from session to session. This challenge has been addressed by the relocalization technique in vivo microcartography, which can relocate structures over multiple days in a variety of tissues, including the lung[58] and melanoma tumours[74].

These techniques are crucial for investigating early stages of tumorigenesis or metastatic seeding, which begin as just a few rare cells stochastically dispersed within an entire tissue. With use of these techniques, the transformation of normal oral tissues into premalignant

and then malignant lesions was visualized by repeated imaging of the entire tongue[75]. In the mammary gland, where epithelial cells are a small and dispersed fraction of the entire tissue, LVHR-IVI captured early dissemination by directly observing single tumour cells escaping the confines of mammary DCIS lesions via intravasation[76]. Finally, in the lung, LVHR-IVI enabled visualization of the arrival and subsequent fate of disseminated tumour cells (DTCs)[77].

Imaging metastatic colonization

One of the earliest uses of IVI to investigate the process of metastatic colonization was that of Wood, who, in 1958, used a transparent chamber implanted into the rabbit ear[78] (developed by Sandison more than 30 years earlier[79]). Wood used this chamber to visualize the fate of tumour cells injected directly into the vasculature.

Since then, metastatic colonization of secondary sites has been investigated in a number of different cancer types and tissues. These studies give a detailed account of the process of metastatic colonization, transforming it from a simple descriptive catch-all phrase into a process that encompasses several individual steps, including cancer cell arrival, extravasation, survival and growth into secondary nodules. In the following subsections, we briefly describe what has been learned to date about the metastatic process using in vivo imaging of various anatomical sites and tissues. Unless otherwise noted, each of the studies mentioned used IVI in one form or another.

Muscle

Early studies of metastasis focused on visualizing the arrival of tumour cells in easily imaged vascularized muscles such as the rabbit ear[78] and the cremaster muscle[80]. However, metastasis of tumours to muscle tissues is very rarely encountered in patients[81]. Skeletal muscle, spleen, thyroid and adipose bone marrow (yellow bone marrow) constitute antimetastatic niches[82], which may be interesting to study to decipher why these sites do not lead to overt metastases. Indeed, recent work studying skeletal muscle (using ex vivo techniques) has determined that, while tumour cells do migrate to muscle, oxidative stress within the tissue creates a microenvironment that prevents outgrowth of these cells[83]. Thus, we may expect further development of imaging windows to study antimetastatic niches in the future.

Lymphatics and lymph nodes

IVI of locoregional dissemination to lymphatics and lymph nodes[84] determined that mechanical pressure placed on tumours can increase tumour cell trafficking to the draining nodes. However, Das et al. showed that, in unperturbed tissues, entry of tumour cells into the lymphatic sinuses occurs through active tumour cell migration and can be prevented by blocking the cytokine receptor C-C motif chemokine receptor 8 (CCR8)[52]. Although development of metastatic foci in lymph nodes (positive lymph nodes) has been associated with worse outcome in patients, it was only recently discovered (using fixed tissue analyses) that cancer cells in positive lymph nodes can migrate haematogenously to distant sites[85-87].

IVI of positive lymph nodes could provide a better understanding of the mechanisms of cancer cell redissemination to distant sites and lead to novel targeted therapies.

Lung

One of the more challenging tissues to image is the lung. Its delicate, yet complex nature has made it a target of imaging since the 1600s[88], with in vivo visualization reported as early as 1925 (ref.[89]). Modifying a vacuum-stabilized imaging window for cats first published in 1939 (ref.[90]), Funakoshi et al. became among the first to image metastatic nodules in the lungs of mice[91]. The group found the vasculature in metastatic nodules to be irregularly shaped compared with normal vessels and to have reduced blood flow[92]. More recently, Headley et al. used this type of imaging window to show that upon arrival in the lung, DTCs fragment and shed tumour microparticles that accumulate in the lung interstitium and generate immune responses[93]. Finally, our group developed an implantable imaging window that allows the mouse to survive, giving multiple views of the lung vasculature for the first time[58,94]. This window can be used to directly visualize the arrival and extravasation of DTCs and follow them as they grow into micrometastases[77]. This work demonstrated that the TME of the primary tumour induces an invasive, stem-like and dormant phenotype within the migrating cancer cells, giving these cells a survival advantage within the metastatic site and the potential to grow into metastatic nodules when the conditions become suitable.

Brain

A similar longitudinal IVI study followed DTCs in the brain over time and observed that DTCs in the brain stop at vascular branch points, extravasate soon after arrival and maintain close contact with the microvasculature[65]. After extravasation, growth of the cancer cells occurred in cancer type-specific patterns, with melanoma metastases using vessel co-option (perivascular growth) and lung cancer-derived metastases forming nodules that induced angiogenesis. Another recent study using serial IVI of the brain showed that escape from dormancy is a rate-limiting step in the development of brain metastases, with astrocytes driving DTC dormancy[95].

In addition to its use for studying patterns of metastatic growth in the brain, IVI could be used to learn more about the mechanisms by which cancer cells break the blood–brain barrier and enter the brain parenchyma. IVI could also potentially help design measures to prevent brain metastases, which are inevitably associated with terminal disease[96].

Liver

One of the first IVI investigations of metastasis in the liver visualized the arrival of fibrosarcoma DTCs, and found cells mechanically trapped in narrow liver sinusoids, without apparent influence from platelets[97]. This was confirmed by Scherbarth and Orr[98], who found that B16 melanoma cells are mechanically trapped in hepatic sinusoids. However, they also found that pretreatment of mice with the pro-inflammatory cytokine interleukin-1α (IL-1α) caused tumour cell adhesion to endothelial surfaces of vessels that were more than twice the size of the tumour cells. Schluter et al.[99] then found that colon carcinoma cell lines had high adhesion rates, independent of their metastatic potential, and that DTCs were

arrested in microvessels with diameters much larger than the adherent tumour cells. These studies demonstrated that in addition to vasculature size, host-derived soluble and cancer cell-intrinsic factors affect metastatic seeding of the liver.

Most recently, Ritsma et al. developed an implantable imaging window for abdominal organs (that is, small intestine, liver, spleen, kidneys and pancreas) and used it to study the steps of colorectal cancer metastasis formation in the liver over the course of 14 days[44,62]. They found that DTCs proliferated to form motile, yet confined, ‘pre-micrometastases’, which then condensed into micrometastases in which cell migration was suppressed and proliferation persisted.

Bone

IVI of metastatic homing to the bone marrow of the calvarium showed that, when injected into the vasculature, most tumour cells (leukaemic, multiple myeloma and prostate) homed to spatially restricted vascular domains within the marrow[100]. Further analysis showed that these domains express stromal cell-derived factor 1 (SDF1; also known as CXCL12), and that benign circulating haematopoietic stem/progenitor cells, mature T lymphocytes, leukaemic cells and tumour cells all extravasate at these locations. Thus, tumour cells use these particular areas of vascular endothelium in a manner that mimics the multistep tissue-homing mechanisms of benign leukocytes. It would be of interest to investigate whether any therapies can target the extravasation of cancer cells at these specific sites without affecting normal physiology.

Summary

Taken together, the studies discussed in this section typify the breadth of applications of IVI, the landmark discoveries that have been made in cancer and metastasis research using IVI, and a vision for the future application of IVI.

Imaging drug action

The development of therapeutics that can prevent or treat metastasis is a major unmet need in cancer research. As IVI can analyse intact tissues that are connected to the systemic circulation, it can be used to track systemically administered drugs, measuring tissue clearance (pharmacokinetics) and the drug’s effect on targeted tissues (pharmacodynamics)[101]. As some therapeutics are administered as prodrugs, which must be metabolized in the body before the intended drug action is achieved[102], they can be studied only in vivo. Standard pharmacokinetics assays involve low-resolution techniques such as blood sampling or tissue homogenization[103]. Pharmacodynamics are usually assessed by histopathology and by low-resolution clinical imaging techniques such as magnetic resonance imaging and positron emission tomography[104]. This leaves the mechanism of action of some therapeutics unknown[105].

A number of IVI investigations have tracked drug distribution and uptake of chemotherapeutics[68,106], nanoparticle drugs[107] and prodrug conjugates[108], targeted therapies[66,109], immunotherapies[67] and radiation sensitization to therapeutics[110]. These

studies show that IVI allows assessment of drug distribution and tissue penetrance, uptake by multiple cell types and evaluation of the resultant cell death, all in real time[31,105,111].

Biosensors

One of the most common uses of IVI has been to visualize and quantify cellular motility. Parameters such as migratory path, velocity, turning frequency and chemotactic index can be extracted from time-lapse videos[112,113]. With multicolour[114,115] and multispectral[116,117] imaging, multiple cell types can also be imaged simultaneously and cell–cell interactions can be visualized and quantified (for example, using interaction times[118]). However, cells, particularly those in tissues, carry a wealth of information that goes beyond motility parameters. Expression of genes, alone or as part of a signature, marks cells as having specific functions or phenotypic states. Use of these genes to drive the expression of fluorescent proteins allows their direct visualization in vivo[119]. This can be particularly important for understanding metastasis and tumour progression.

Imaging of phenotypic states of cells

It has been postulated that a stem cell-like phenotype is needed for metastatic colonization. However, given the plasticity of DTCs, the exact location where stemness induction occurs along the metastatic cascade has been difficult to ascertain. With use of an inducible fluorescent colorectal carcinoma model designed to intravitally visualize cancer stem cells (CSCs; cells that express leucine-rich repeat-containing G protein-coupled receptor 5 (LGR5)), it was recently demonstrated that disseminated colorectal cancer cells retain a non-stem-like, highly motile phenotype (and are $LGR5^{-}$) while in the circulation and during colonization of distant organs (liver)[120]. However, these cells possess intrinsic plasticity and can switch to become $LGR5^{+}$ cells in response to microenvironmental factors produced at secondary sites, such as hepatocyte growth factor (HGF) and fibroblast growth factor 2 (FGF2). Furthermore, selective ablation of $LGR5^{+}$ cells prevented metastatic outgrowth, confirming that a stem-like phenotype is required for the initiation of metastatic outgrowth in this model.

Contrary to the reduction of stemness during dissemination found in colorectal cancer, recent IVI analysis of breast cancer using a biosensor for stemness[121] found that a stem-like phenotype is enriched within specific microanatomic locations of the primary tumour that contain intravasation portals, called ‘tumour microenvironment of metastasis (TMEM) doorways’[41]. That study found that the density of CSCs is further enriched during metastatic dissemination, with CSCs making up more than 60% of circulating cancer cells. This stemness phenotype persists during cancer cell arrival at a distant organ (the lungs) and early metastasis formation, and then decreases as metastatic nodules increase in size. Tracking the fate of DTCs upon arrival in the lungs with IVI through implantable lung imaging windows shows that these spontaneously disseminating cancer cells also exhibit invasive and dormant phenotypes, which provide extravasation and survival advantages[77].

Thus, it seems that the need for activation of a programme of stemness during the metastatic cascade is cancer type specific and target organ specific. However, in both studies, non-CSCs displayed higher migration velocities than CSCs, indicating that some properties

of CSCs are universal across cancer types. Further investigation using IVI should allow delineation of therapeutic targets to block stemness induction and exit from dormancy.

Imaging of oxygen tension and hypoxic tumour cells within the TME

Oxygen tension and pH can affect both cancer progression and response to treatment. Although one would expect that these parameters correlate with each other (for example, hypoxic areas exhibit low pH), a study by Jain and colleagues using high-resolution imaging combined with fluorescence ratio imaging microscopy and phosphorescence quenching microscopy showed that no such correlation exists, demonstrating an extraordinarily complex connection between perfusion and metabolism within the TME[122]. Although these studies were performed intravitally using human colon carcinoma cells, the microenvironment was potentially not reflective of that in human tumours as the xenografts were grown ectopically in a dorsal skin fold chamber, which may have a microenvironment substantially different from the one these cells encounter physiologically.

Despite this limitation, discrepancies between areas of high oxygen tension and expected high intracellular oxygenation were also observed at the single-cell level by real-time IVI of orthotopically implanted breast cancer cells. This was accomplished using tumour cells expressing a novel hypoxia biosensor that is sensitive to the expression of hypoxia-inducible factor 1 α (HIF1α)[39]. The study showed that hypoxic tumour cells can paradoxically be found located adjacent to well-perfused blood vessels. Furthermore, it showed that metabolically hypoxic cells display an invadopodium-rich, slow migratory phenotype with enhanced matrix degradation activity that is characteristic of migrating cancer cells[123].

Imaging of apoptotic cell death

Observing cancer cell death within the native TME can be useful to determine the effect of drugs on apoptosis. BODIPY-labelled peptides that bind to apoptotic cells in a Ca^{2+}-independent manner and fluoresce in green (Apo-15 (ref.[124])) or red (Apotracker Red[125]) may be useful to study the effects of experimental therapeutics on cancer cells in their native microenvironment. These studies would be of higher fidelity than studies performed in vitro, and could help understand which cells within the TME become therapy resistant and which drugs can alleviate this resistance.

Imaging of intrinsic signals

In addition to biosensors, signals that are native to the tissue, such as second-harmonic generation signal[126] or autofluorescence, can provide useful information. Fluorescence lifetime imaging measures the time of arrival of individual photons after pulsed excitation of auto-fluorescent molecules such as NADH and FAD[127]. While the arrival time of each photon is stochastic, the distribution of arrival times follows an exponential decay, with the characteristic decay time dependent on the chemical microenvironment surrounding the fluorescent molecule[38]. Intravital fluorescence lifetime imaging has been used to investigate cell type-specific metabolic signatures[128-130], and therapeutic responses[131]. Use of intrinsic signals greatly simplifies experiments and makes possible the extension of IVI tools to clinical applications (where exogenous labelling of tissues is not possible)[132,133].

Imaging metastatic dissemination

Understanding how tumour cells intravasate is critical for discovering approaches to decrease overall metastatic burden. Blocking intravasation could be used for patients with local and regional disease who receive systemic preoperative (neoadjuvant) therapies, which, in certain instances, may increase haematogenous dissemination[69,134]. In addition, blocking dissemination may still be important in patients who had their primary tumour resected, because evidence is accumulating that haematogenous dissemination also occurs from metastatic lesions[135,136]. Indeed, the relative number of circulating tumour cells is an important prognostic and predictive factor in metastatic breast[137], colon[138,139] and pancreatic[140] cancers.

Despite the importance of understanding how tumour cells gain access to the blood vasculature, there is considerable debate regarding the answer to this question. Two (not mutually exclusive) theories exist: that of collective migration followed by collective vascular invasion, and that of single-cell and streaming (coordinated single-cell) migration, followed by single-cell intravasation.

Evidence for collective migration

The concept of collective migration[141] dates to early observations of the motility of tumour cells grown in 3D matrices in vitro. These studies noted that small clusters of cells can move together in vitro[142] and grow in ‘ribbons’, reminiscent of tumour cell aggregates observed embedded in connective tissue in histological sections of patient tumours[143]. However, only three studies have directly observed collective migration in vivo in orthotopically injected tumour cells[144-146]. Of these three studies, Giampieri et al.[144] found that collective migration was not associated with haematogenous dissemination but was instead observed during cancer cell invasion into lymphatic vessels.

These studies[144-146] used tumour cell lines that fail to recapitulate the histology and progression of cancers observed clinically. IVI studies in transgenic mouse models of cancer, which do follow the clinical disease progression and histology[147,148], have not observed collective migration, nor have they observed that migrating tumour cells need to invade the stroma for them to intravasate. Indeed, by study of whole-mount excised tumour tissues to evaluate the quantity and location of intravasation sites across the entire tissue (tumour and adjacent stroma), it was determined that more than 98% of intravasated cells are found at the tumour interior, not in the stroma[149]. This result is consistent with the findings of studies using IVI[64] and immunohistopathology[85,150-152].

While patterns of tumour cells extending into the stromal tissue that are consistent with those observed in 3D in vitro assays have been observed histologically in fixed tissues from mice[153] and humans[154], it is impossible to determine from fixed tissues whether these patterns arose from the collective migration of tumour cells or from asymmetrical tumour cell division and growth. Still, both tumour strands[154] and tumour buds (single or small tumour cell clusters (four cells or fewer))[155,156] found at the invasive tumour front correlate with clinical outcome in patients. It is possible that these histological patterns are related to an advanced stage of tumour progression, but not necessarily collective migration.

Finally, collective migration can be a mode of tumour cell dissemination only if, as speculated, it leads to the collective vascular invasion of tumour cells. Evidence supporting collective vascular invasion stems only from analysis of fixed haematoxylin and eosin-stained mouse and human tissue sections, which is a method incapable of distinguishing between lymphatic vasculature and blood vasculature[157]. Most importantly, it has since been determined by immunostaining that in more than 97% of cases of intravascular tumour clusters, the vessels are lymphatic vessels, not blood vessels[158].

The observation of tumour cell clusters[159-161] in the circulation of mice and human patients has also been used to support the hypothesis of collective migration and collective vascular invasion. However, those studies used non-physiological conditions to promote cell cluster generation and may reflect tissue damage rather than dissemination ability. Thus, although recent work seems to indicate that tumour cell clusters in the lung are more potent at generating metastases than single tumour cells[162], direct evidence for this conclusion and the origin of cell clusters is still lacking. Invasion of cohesive clusters of tumour cells directly into the blood vasculature, as inferred from cell clusters detected in peripheral blood, has, to our knowledge, never been seen by IVI.

The paradox that single tumour cells enter the blood, but that tumour cell clusters seed distant metastases, may be resolved by the finding that tumour cell cluster formation is associated with CD44-mediated intercellular adhesion[163]. This additionally increases DTC survival and improves DTC seeding as CD44 is associated with a CSC phenotype[164]. Consistent with this finding are the observed stem-like gene expression patterns of tumour cell clusters found in the blood circulation in live mice[165]. Together, these results support a pattern of dissemination where single tumour cells intravasate and subsequently form clusters (supported by gene expression patterns associated with stemness) in the circulating blood.

Evidence for single-cell/streaming migration during dissemination

Multiphoton IVI has played a major role in defining the mechanism of single tumour cell dissemination. IVI by our group[64,123,166-169], and by others[144,148,170], has established that (1) single-cell and streaming migration are seen frequently in invasive carcinoma in a variety of mouse models, including transgenic, xenograft and tissue transplant models[64,123,144,148,166-170]; (2) macrophages are essential to this process[64,168]; and (3) these single-cell migration patterns of tumour cells and macrophages are associated with haematogenous dissemination[64,167,169]. Even at secondary sites such as the lung, our IVI studies[57,58], and ex vivo imaging studies by others[171,172], have demonstrated the involvement of macrophages in the extravasation of tumour cells.

IVI of mammary tumours has been used to observe that, during streaming migration, solitary tumour cells and macrophages communicate with each other via a paracrine interaction[173] and move together (as unattached cells at speeds of 10–100 times the speeds commonly seen in similar cell types in vitro[123,166,168]) along collagen fibres towards blood vessels[168]. Macrophage–tumour cell interactions in the migrating stream alter gene expression in the tumour cells in a pattern called the ‘invasion signature’[174]. One of the most highly altered proteins in this signature[175] is the actin-regulatory protein MENA (also known as ENAH),

which has several splice variants[176]: MENA11a (associated with an epithelial phenotype) is downregulated during streaming migration, and MENA^{INV} (an isoform that leads to higher levels of motility and increased sensitivity to growth factors such as epidermal growth factor (EGF)[166], HGF[177] and insulin-like growth factor (IGF)[178]) is overexpressed. Another change in the MENA-specific expression pattern, MENA^{Calc}, reflects the relative amount of MENA11a compared with total MENA levels and is prognostic for risk of metastatic recurrence in patients with breast cancer[179,180].

Evidence for cancer cell intravasation portals

IVI of mammary carcinomas has revealed that once the streams of macrophages and tumour cells reach the vasculature, they slow down and associate with TMEM doorways. TMEM doorways are composed of one macrophage expressing high levels of the receptor tyrosine kinase TIE2 (also known as TEK) and vascular endothelial growth factor (VEGF), one MENA-expressing tumour cell and one endothelial cell, all in direct and prolonged stable contact[64,151,168,181]. Long-duration time-lapse multiphoton IVI has shown that the TMEM doorways themselves are stable over extended periods, during which they regulate transient, localized blood vessel opening and cancer cell entry into the bloodstream[64,169]. IVI has been used to directly visualize single-cell intravasation through these doorways in several transgenic and xenograft mouse models of breast cancer[64,76,114,168].

Active TMEM doorways are found in pre-invasive[76,167] and invasive ductal[64] breast cancer as well as in metastatic foci in lungs[58] and positive lymph nodes[152], indicating that TMEM doorway-mediated cancer cell dissemination occurs not only at the primary tumour site but also at metastatic sites, which could perpetuate metastatic dissemination even after removal of the primary tumour. The observation of TMEM doorways in lymph nodes supports indirect studies that have concluded that tumour cell dissemination from lymph nodes occurs via a haematogenous route[85,87,182].

Recent work using IVI with CSC biosensors and immunofluorescence of fixed tissues has shown that TMEM doorways are microenvironments enriched in CSCs and MENA^{INV}-expressing cancer cells owing to increased cancer cell–macrophage contact that occurs around TMEM doorways[41]. This work provides an explanation as to why tumour cells crossing into the blood circulation are CSCs, and why tumour cells that make contact with macrophages around TMEM doorways exhibit greatly enhanced transendothelial migration activity (a consequence of MENA^{INV} expression increasing their ability to enter the blood circulation[183]). Thus, this observation provides the mechanism through which single breast tumour cells entering the blood may lead to tumour cell clusters seeding distant metastases; macrophages are responsible for increased intercellular adhesion (CD44 expression leading to clustering in the blood), and the induction of a stem-like phenotype, leading to enhanced tumour-initiating capacity.

The observation that tumour cells migrate from metastatic nodules[85-87,135], and that metastasis-to-metastasis seeding is a common event[184,185], indicates that it would not be too late to inhibit TMEM doorway function after removal of the primary tumour. This is because, in some patients, cancer cells might have already migrated from the primary site

and formed clinically undetectable micrometastases, which could be a source of further metastatic tumour cell dissemination and could increase overall metastatic burden.

Indeed, IVI showed that a TIE2-specific inhibitor, rebastinib, can inhibit TMEM doorway-associated vascular opening and intravasation[69,186]. Rebastinib substantially decreases the numbers of circulating tumour cells in mice and humans with breast cancer[69,186,187]. Furthermore, mice with metastases from a mammary tumour survive after tumour resection and treatment with rebastinib plus cytotoxic chemotherapy, whereas those treated with resection and chemotherapy alone do not[186]. As discussed further later, rebastinib is currently in phase I clinical trials for use in breast cancer and other cancers[188,189].

Clinical translation of IVI findings

Biomarkers for metastasis

Some of the discoveries pertaining to the metastatic cascade made by IVI have been successfully translated to the clinic in the form of biomarkers capable of prognosticating metastatic recurrence in patients[150,151,179-181,190]. In particular, the density of TMEM doorways is significantly associated with distant recurrence, specifically early recurrence (5 years after diagnosis)[181], and MENA^{Calc} has been positively associated with the risk of death in three breast cancer cohorts[179,180], independent of other traditionally measured clinical parameters.

These retrospective studies[150,151,179-181], which comprise thousands of patients, demonstrate how insights gained from IVI can yield prognostic tests specific for metastatic dissemination. Further, the fact that tests such as the TMEM doorway score have a very poor correlation with assays that measure proliferation (for example, Oncotype DX Breast Recurrence Score) confirms that a distinct biological process is being measured by the TMEM doorway-related prognostics[181] (Box 4). These new prognostics that specifically measure the process of dissemination should enable the evaluation of a new class of desperately needed antidissemination drugs[69,186,187,191].

Effect of therapy on the TME as seen by IVI

IVI has been used to demonstrate the effects of systemic therapies (for example, chemotherapy, radiotherapy, targeted therapy and anti-angiogenic therapy) on the TME (Fig. 3), a phenomenon known as the host response[192]. Changes in the TME of the primary tumour and metastatic sites (for example, influx of bone marrow-derived progenitors or modulation of immune response within the primary tumour) can influence drug delivery, cancer progression, cancer dissemination and drug resistance.

Systemic therapy depends on drug delivery into the TME (a dynamic process best studied in vivo). Numerous important conclusions regarding drug delivery have been made with the help of IVI. IVI has shown that tumour vasculature is permeable to subcellularsized nanoparticles[193,194], leading to the concept of increased vascular ‘leakiness’ in tumour beds, and associating this leakiness with poor therapeutic delivery[195]. However, increased vascular permeability may be beneficial for the selective delivery of chemotherapeutics into, and their retention in, tumour interstitial tissues, an effect termed ‘enhanced permeability

and retention' (EPR)[196,197]. While EPR is primarily associated with solid tumours, there is evidence that nanocarriers can enhance the interaction of therapeutics with lymphoma cells[198]. This demonstrated that drug delivery into tumours can be improved via vascular disruption of intratumoural blood vessels. This is accomplished using the recently developed technique of acoustic vaporization and the application of microparticle- and nanoparticle-carrying drugs[199].

IVI has also revealed that, in breast cancer, radiotherapy and chemotherapy can induce transient vascular disruption (depending on perivascular macrophage density)[110]. In particular, perivascular macrophages elicit dynamic bursts of serum extravasation, enhancing delivery of nanoparticles and subsequently increasing drug uptake in neighbouring tumour cells (Fig. 3a). Moreover, combining radiotherapy with the chemotherapy cyclophosphamide increased macrophage influx and delivery of nanoparticles further, suggesting that conventional anticancer therapies may be used to prime the TME for drug delivery[110]. Similarly, other groups demonstrated that chemotherapy increases the density of perivascular TIE2^{hi} macrophages and TMEM doorways, and increases TMEM doorway opening[69,110,134] (Fig. 3a). These changes, along with a chemotherapy-induced increase in MENA^{INV} expression in primary breast tumours, contribute to increased vascular opening that is linked to cancer cell dissemination and metastatic seeding at secondary sites[69,134]. This chemotherapy-promoted TMEM doorway assembly and function[69] is suppressed by rebastinib, which targets TMEM TIE2^{hi} macrophages[69,186].

The aforementioned observations may be a part of essentially the same biological phenomenon: a TME response resulting from a chemotherapy-mediated increase in the density of perivascular macrophages. It would be interesting to investigate whether drug delivery can be improved in the clinic by exploiting macrophage-induced vascular opening in the TME upon radiotherapy and cytotoxic chemotherapy, as suggested by Miller et al.[110], while at the same time suppressing the TMEM doorway-associated increase in tumour cell dissemination.

IVI has shown that, in breast cancer, the tumour's response to chemotherapy, as well as the delivery of chemotherapeutics, depends on tumour size[68], demonstrating that chemotherapy increases macrophage density in the TME, which subsequently hampers a beneficial response of the tumour to chemotherapy (Fig. 3a). Another IVI study showed the effect of chemotherapy on the induction of dormancy and the protective effect of osteopontin on dormant acute lymphoblastic leukaemia (ALL) cells in mice[200]. Using a cranial imaging window, the researchers demonstrated that multiple rounds of chemotherapy result in minimal residual disease, which is refractory to treatment, and that treatment response can be increased by injection of osteopontin-targeting antibodies.

IVI was also used to understand the response of certain solid tumours to targeted therapy. For example, IVI of an ERK/MAPK biosensor was used to study mechanisms underlying the resistance of melanoma cells carrying a *Braf* mutation to anti-BRAF therapies[201] (Fig. 3b). Specifically, tolerance to the BRAF inhibitor PLX4720 developed rapidly in a TME with high stromal density. Mechanistically, PLX4720 activates melanoma-associated fibroblasts, leading to increased matrix production and elevated integrin β1–focal adhesion

kinase (FAK)–SRC signalling to ERK in melanoma cells. Co-inhibition of BRAF and FAK decreased tumour size by abolishing PLX4720-induced ERK activation and resensitizing melanoma cells to BRAF inhibition.

Furthermore, IVI has been used to study the effect of targeted therapy on the most common types of leukaemia, acute myeloid leukaemia (AML) and T cell ALL (Fig. 3c) and helped explain the disappointing results from clinical studies of patients with AML treated with C-X-C motif chemokine receptor 4 (CXCR4) inhibitors. Visualization of the effect of the CXCR4 inhibitor AMD3100 on the motility of AML cells and T cell ALL cells indicated that AMD3100 inhibited retention of ALL cells within the bone marrow niche (which is supportive of a chemo-resistant phenotype) but AML cells were still retained within the niche, most likely owing to compensatory signals from other chemokines, such as C-C motif chemokine ligand 2 (CCL2)[202]. Thus, IVI contributed mechanistic information critical for guiding clinical trials in patients with leukaemia. The same group previously used a similar IVI approach to demonstrate that the dynamic interactions of T cell ALL with the bone marrow microenvironment are responsible for refractory disease[203]. This helped redirect the clinical therapeutic strategy of combating chemo-resistant T cell ALL from targeting the bone marrow stroma to targeting cell migration and the interaction of cells with the bone marrow niche.

IVI was also instrumental in evaluating the role of anti-angiogenic therapy in melanoma; this therapy facilitated tumour infiltration of lymphocytes, which led to an adaptive immune response and a reduction in tumour growth in mice with subcutaneously grown B16 melanoma[204] (Fig. 3d). Mechanistically, this work exploited the observations that the expression of endothelial adhesion molecules (for example, vascular cell adhesion molecule 1 (VCAM1)) is crucial for leukocyte extravasation, and that the expression of endothelial adhesion molecules can be suppressed by proangiogenic factors such as VEGF. Indeed, using IVI, the researchers visualized the promoting effect of anti-angiogenic therapy on vascular rolling, adherence and transmigration of leukocytes into the melanoma microenvironment, which increased the effectiveness of adoptive immunotherapy.

In addition to evaluating the effect of various therapies on the TME of primary tumours, IVI was used to assess the response of cancer cells to chemotherapy in metastatic sites. IVI through an abdominal imaging window indicated that, regardless of the type of chemotherapeutic used, liver-metastatic colon carcinoma cell lines show similar changes such as cell fragmentation, condensation, swelling and intracellular vacuoles[205]. This indicates that cytotoxic chemotherapy induces nonspecific tissue damage and explains why a similar host response can be observed, regardless of chemotherapy[206-209]. Likewise, IVI was used to follow the fate of colon cancer cells migrating from spleen to liver. That study followed, at the single-cell level, the effect of 5-fluorouracil on cancer cell adhesion to endothelial cells in liver sinusoids, as well as the cytotoxic effect of 5-fluorouracil on early metastases (4–10 days after intrasplenic tumour injection) and late metastases (2–8 weeks after intrasplenic injection). 5-Fluorouracil did not affect cancer cell extravasation, but showed cytotoxic activity at early and late stages of metastasis[210].

In summary, IVI has substantially contributed to our understanding of the tumour–host interaction during various anticancer treatment modalities. These insights should enhance our ability to successfully treat patients with advanced cancer.

Future perspectives

Limitations of IVI

Despite advances that have made IVI more accessible and versatile, several limitations still hamper widespread adoption of the technique. These include limitations on imaging depth; garnering information on cellular identity and functional state; the ability to control experimental conditions; and image analysis. In this section we present some of the initial attempts to address these shortcomings and lay out the need for further development.

Increasing depth of penetration

Although still extremely shallow compared with clinical imaging techniques, multiphoton imaging provides some of the greatest penetration depths compared with other optical microscopy techniques, with an approximate twofold to fivefold increase over confocal microscopy[211,212]. The ultimate depth of penetration of multiphoton microscopy varies greatly with the scattering properties of the imaged tissue. Relatively uniform tissues such as brain offer the greatest depth of penetration (~500 μm), while those consisting of multiple layers of lipid–water–air interfaces (such as the lung) rapidly destroy the illumination's point spread function (a crucial parameter for multiphoton signal generation) and limit imaging depth (~30 μm).

Attempts to increase this limit have mainly focused on reducing tissue scattering by increasing the wavelength of illumination and/or emitted light. Thus, the development of far-red fluorophores has been an active area of research[213-216], and has motivated the push to extend the wavelength range of multiphoton microscopes by using pulsed light sources that can efficiently excite them (for example, using optical parametric oscillators[114,217], fibre lasers[218] or three-photon excitation[219]). More recently, another tack has been to try to compensate for the point spread distortions using adaptive optics with two-photon[220-222], three-photon[223] and even four-photon[224] excitation. These techniques have extended the depth of penetration for some tissues (such as brain) to more than 1 mm (ref.[225]).

Correlative IVI

Multiphoton microscopy is excellent at revealing the behaviour and dynamics of cells and tissues. However, structures that lack fluorescence- or harmonic-generating molecules do not produce any optical signal, and thus do not appear in acquired images. Histochemistry and immunostaining, on the other hand, are extremely versatile in their ability to label cells and structures, but, as they require fixation and mechanical sectioning of tissues, they can give only single time point snapshots and cannot capture cellular or tissue dynamics.

To overcome these limitations, two groups have developed methods for mechanically sectioning the fixed tissue after IVI to capture the cells contained within the IVI plane of focus for further analysis by fixed–frozen histochemistry and immunostaining[226] or

by electron microscopy[227,228]. Although limited by their labour-intensiveness, and by the small number of cells (~5–10) that can be correlated, these techniques hold the promise to link behavioural phenotypes with cellular, molecular and ultrastructural identity and composition. Improved methods that can increase throughput, as well as the number of aligned cells by orders of magnitude, are still needed.

Combination with other preclinical research modalities

A wealth of information can be obtained by the rapidly advancing methods for accessing and analysing the DNA, RNA, protein, lipid and metabolite content of cells. Powerful techniques capable of extracting information on limited numbers of targeted analytes (for example, limited sets of genes, transcripts, proteins and so on) are now being expanded into ‘omics technologies for unbiased discovery-based research[229,230]. As originally developed, many of these approaches required the isolation and destruction of cells and tissues during the analysis, resulting in loss of their original spatial relation to other cells in the tissue. However, recent advances have made it possible to perform these analyses while preserving the architecture of the tissues. Mass spectrometry imaging[231], multiplexed fluorescence in situ hybridization[232], highly multiplexed immunohistochemistry[233] and immunofluorescence[234], and spatial transcriptomics and proteomics[232] could all be readily combined with IVI, and we expect such combinations to lead to new insights into mechanisms of metastasis.

Functional imaging

Even with the advantages that correlative microscopy provides, the aforementioned techniques still deliver information on the state of the cells at single time points. While advances have been made in the design and use of fluorescent reporters and biosensors, without more sophisticated methods for manipulating cells in vivo, IVI remains largely an observational and correlative technique.

Conventional methods for studying molecular mechanisms in vivo use approaches where gain-of-function and loss-of-function experiments are affected either via the systemic application of drugs or via the genetic manipulation (constitutively or chemically induced) of germline cells or somatic cells introduced into naive host animals. While powerful, these approaches lack the spatial and temporal control to precisely target cells without unwanted on-target and off-target side effects.

To truly realize the goal of performing in vivo studies that can define and test molecular mechanisms at single-cell resolution, in real time and longitudinally, researchers need to experimentally manipulate cellular processes locally and transiently, all in a native tissue context that is connected to the lymphatic and cardiovascular circulatory systems (which could, for example, provide immune infiltrates). The field of optogenetics (the combination of genetics and optics to control protein function with light[235]) holds the promise of fulfilling this need. The past two decades have seen an enormous growth in the number and variety of optogenetic tools that can regulate cellular processes[236-238].

Optogenetic tools now exist to control a variety of cellular functions, including membrane potentials (via light-controlled ion channels and pumps)[239], enzymes[240], signalling

receptors[241], protein activity (by controlling protein localization[242] or binding[243]), and gene expression[244] and repression[245]. Despite these advances, the use of optogenetic tools in vivo has mainly been in neuroscience applications[237], although use is increasing in cardiovascular research[246] and developmental biology[247]. Since new CRISPR technologies are greatly simplifying the incorporation of optogenetics into mouse models[248,249], the main stumbling block to widespread adoption of optogenetics is the slow and often complex illumination schemes that are required to activate processes such as transcription. Miniaturized wearable light-emitting electronic devices are now being developed, although almost exclusively for neuroscience applications[250-253].

Artificial intelligence and deep learning

Finally, one of the major bottlenecks for IVI experiments is image analysis, which has been limited to manual (or at best semi-automated) techniques. This is because, unlike images of in vitro cultures, where cells can be sparse and easily separated, cells in tissues are closely packed, and often of similar intensities. The lack of fully automated analyses is particularly problematic when time-lapse IVI or LVHR-IVI is used, as these techniques generate voluminous amounts of data, making better machine vision algorithms sorely needed. Very few investigations have used artificial intelligence on IVI data to date[254,255], although efforts are under way to establish databases of IVI images[256], a crucial prerequisite for the development of machine learning algorithms.

Furthermore, IVI images present a wealth of data that may not be easily interpretable without a better understanding of the behaviour of cells within tissues. Thus, application of artificial intelligence or deep learning techniques may enable the discovery of hidden phenotypes[123,257] that are predictive of cellular behaviours under specific stimuli, or within specific microenvironmental niches.

Conclusions

There is a consensus that the TME determines tumour phenotype and response to treatment in ways that transcend the genetic mutations that drive tumour growth. Understanding the mechanisms behind the role of the TME requires real-time and longitudinal observations in living animals at single-cell resolution. Multiphoton IVI has now progressed to the stage where it can be relied on as a major tool in the effort to study the TME and its role in the host response.

New technologies can be used to define clinically actionable mechanisms responsible for tumour cell dissemination and metastatic recurrence, and can overcome previous obstacles to visualizing tumour cell motility phenotypes in vivo. These technologies have allowed the visualization of the tumour cell migration phenotypes associated with tumour cell dissemination and metastasis, including the intravasation of single tumour cells, de novo tumour cell cluster formation inside blood vessels and extravasation at metastatic sites. They also hold the promise of resolving remaining paradoxes in the literature regarding the relative contributions of single-cell migration and intravasation compared with collective migration and collective vascular invasion. IVI has led to the discovery of TMEM doorways involved in dissemination of tumour cells at both primary tumours and metastatic sites, and

new prognostics and treatment options for use in combating distant metastatic recurrence in patients with breast cancer. IVI has also given direct insights, at single-cell resolution, into the effects of systemic therapies on, and the contribution of the microenvironment to, the host response.

Finally, IVI has played a central role in elucidating the mechanisms underlying clinically observed therapy failures, in particular those associated with changes in the TME, and has additionally pointed to optimal drug combinations that can overcome this failure. As interactions between cancer cells and the TME are often dynamic, IVI will continue to be the method of choice to understand how cancer cells behave in their natural environment, longitudinally during cancer progression and in response to treatment.

Acknowledgements

This work was supported by the Gruss Lipper Biophotonics Center and the Integrated Imaging Program at Albert Einstein College of Medicine, the EGL Charitable Foundation and grant number CA216248.

Glossary

Acoustic vaporization
Vascular disruption induced by vaporization of microscale or nanoscale droplets using ultrasound sonication.

Chemotactic index
A metric capable of measuring the directed movement of an organism or entity in response to a chemical stimulus.

Collective migration
The coordinated movement of a large cluster of adherent tumour cells that retain homotypic cell–cell junctions out of the tumour mass and towards the stromal blood vasculature.

Confocal microscopy
A form of high-resolution optical microscopy that captures optical sections with single-cell resolution by collecting light only from a single slice of an otherwise intact tissue.

Fluorescence ratio imaging microscopy
An optical microscopy technique that measures the ratio of two different wavelengths to quantify shifts in the fluorescence spectra of probes without the influence of system-specific parameters (for example, detector quantum efficiency, excitation intensity and optical path length).

Liver sinusoids
Highly specialized endothelial cells forming fenestrated blood vessels of the hepatic microcirculation.

Machine vision
Imaging-based automatic inspection and analysis.

Magnetic resonance imaging

A relatively low resolution but deeply penetrating imaging technique, commonly used in the clinic, which measures the effect of strong magnetic fields on the nuclei of water molecules to form an image of the structure, and sometimes function, of tissues and organs.

Mosaicked pattern
A combination or merger of multiple high-resolution, high-magnification images of a sample into a single image, producing a low-magnification, high-resolution image.

Multiphoton microscopy
A form of optical microscopy that captures optical sections with single-cell resolution by using femtosecond pulsed lasers to limit signal generation to a single slice of an otherwise intact tissue.

Optical sections
Images of a single thin plane from within a thick sample captured by removal of out-of-focus light. The name originates from the similarity these images have to those obtained from mechanically sectioned and stained tissues.

Phosphorescence quenching microscopy
In the biological sciences, an optical microscopy technique for the sensitive evaluation of oxygen consumption using optical oxygen sensors whose phosphorescence changes with oxygen concentration.

Point spread function
The 3D diffraction pattern of light formed at the focus of a lens.

Positron emission tomography
A low-resolution but deeply penetrating imaging technique, commonly used in the clinic, which forms images of the physiological function (blood flow, metabolism, neurotransmitters and drug accumulation) of organs using the emissions of an intravenously injected radioactive drug (called a ‘tracer’).

Second-harmonic generation signal
Light originating from second-order non-linear optical scattering by non-centrosymmetric molecules such as collagen or microtubules.

Vessel co-option
The ability of tumour cells to incorporate pre-existing vessels from surrounding tissues, rather than using angiogenesis.

References

1. Chaffer CL & Weinberg RA A perspective on cancer cell metastasis. Science 331, 1559–1564 (2011). [PubMed: 21436443]
2. Pantel K & Brakenhoff RH Dissecting the metastatic cascade. Nat. Rev. Cancer 4, 448–456 (2004). [PubMed: 15170447]
3. Warren S & Gates O The fate of intravenously injected tumor cells. Am. J. Cancer 27, 485–492 (1936).

4. Seruga B, Ocana A, Amir E & Tannock IF Failures in phase III: causes and consequences. Clin. Cancer Res 21, 4552–4560 (2015). [PubMed: 26473191]
5. Jardim DL, Groves ES, Breitfeld PP & Kurzrock R Factors associated with failure of oncology drugs in late-stage clinical development: a systematic review. Cancer Treat. Rev 52, 12–21 (2017). [PubMed: 27883925]
6. DeClerck YA, Pienta KJ, Woodhouse EC, Singer DS & Mohla S The tumor microenvironment at a turning point knowledge gained over the last decade, and challenges and opportunities ahead: a white paper from the NCI TME network. Cancer Res. 77, 1051–1059 (2017). [PubMed: 28209610] This article reports the consensus view of the Tumor Microenvironment Network, a 10-year-long US National Cancer Institute-funded programme aimed at investigating tumour–host interactions in different organ systems, and its finding that tumour–stroma interactions play an important role in tumour progression and metastasis.
7. Eddy RJ, Weidmann MD, Sharma VP & Condeelis JS Tumor cell invadopodia: invasive protrusions that orchestrate metastasis. Trends Cell Biol. 27, 595–607 (2017). [PubMed: 28412099]
8. Condeelis J & Weissleder R In vivo imaging in cancer. Cold Spring Harb. Perspect. Biol 2, a003848 (2010). [PubMed: 20861158]
9. Beerling E, Ritsma L, Vrisekoop N, Derksen PW & van Rheenen J Intravital microscopy: new insights into metastasis of tumors. J. Cell Sci 124, 299–310 (2011). [PubMed: 21242309]
10. Zipfel WR, Williams RM & Webb WW Nonlinear magic: multiphoton microscopy in the biosciences. Nat. Biotechnol 21, 1369–1377 (2003). [PubMed: 14595365]
11. So PT, Dong CY, Masters BR & Berland KM Two-photon excitation fluorescence microscopy. Annu. Rev. Biomed. Eng 2, 399–429 (2000). [PubMed: 11701518]
12. Hoffman RM The multiple uses of fluorescent proteins to visualize cancer in vivo. Nat. Rev. Cancer 5, 796–806 (2005). [PubMed: 16195751]
13. Pittet MJ & Weissleder R Intravital imaging. Cell 147, 983–991 (2011). [PubMed: 22118457]
14. Weigert R, Porat-Shliom N & Amornphimoltham P Imaging cell biology in live animals: ready for prime time. J. Cell Biol 201, 969–979 (2013). [PubMed: 23798727]
15. Peti-Peterdi J In vivo microscopy. Nephrol. Ther 12 (Suppl. 1), 21–24 (2016).
16. Perrin L, Bayarmagnai B & Gligorijevic B Frontiers in intravital multiphoton microscopy of cancer. Cancer Rep. 3, e1192 (2020).
17. Vaghela R, Arkudas A, Horch RE & Hessenauer M Actually seeing what is going on - intravital microscopy in tissue engineering. Front. Bioeng. Biotechnol 9, 627462 (2021). [PubMed: 33681162]
18. Condeelis J & Segall JE Intravital imaging of cell movement in tumours. Nat. Rev. Cancer 3, 921–930 (2003). [PubMed: 14737122]
19. Chishima T et al. Cancer invasion and micrometastasis visualized in live tissue by green fluorescent protein expression. Cancer Res. 57, 2042–2047 (1997). [PubMed: 9158003]
20. Naumov GN et al. Cellular expression of green fluorescent protein, coupled with high-resolution in vivo videomicroscopy, to monitor steps in tumor metastasis. J. Cell Sci 112, 1835–1842 (1999). [PubMed: 10341203]
21. Farina KL et al. Cell motility of tumor cells visualized in living intact primary tumors using green fluorescent protein. Cancer Res. 58, 2528–2532 (1998). [PubMed: 9635573]
22. Hoffman RM & Yang M Subcellular imaging in the live mouse. Nat. Protoc 1, 775–782 (2006). [PubMed: 17406307]
23. Yang M et al. Dual-color fluorescence imaging distinguishes tumor cells from induced host angiogenic vessels and stromal cells. Proc. Natl Acad. Sci. USA 100, 14259–14262 (2003). [PubMed: 14614130]
24. Hoffman RM & Yang M Color-coded fluorescence imaging of tumor-host interactions. Nat. Protoc 1, 928–935 (2006). [PubMed: 17406326]
25. Alieva M, Ritsma L, Giedt RJ, Weissleder R & van Rheenen J Imaging windows for long-term intravital imaging: general overview and technical insights. Intravital 3, e29917 (2014). [PubMed: 28243510]

26. Kitamura T, Pollard JW & Vendrell M Optical windows for imaging the metastatic tumour microenvironment in vivo. Trends Biotechnol. 35, 5–8 (2017). [PubMed: 27238900]
27. Entenberg D et al. Imaging tumor cell movement in vivo. Curr. Protoc. Cell Biol 10.1002/0471143030.cb1907s58 (2013).
28. Ritsma L, Ponsioen B & van Rheenen J Intravital imaging of cell signaling in mice. Intravital 1, 2–10 (2012).
29. Timpson P, McGhee EJ & Anderson KI Imaging molecular dynamics in vivo-from cell biology to animal models. J. Cell Sci 124, 2877–2890 (2011). [PubMed: 21878495]
30. Zomer A et al. Intravital imaging of cancer stem cell plasticity in mammary tumors. Stem Cell 31, 602–606 (2013).
31. Miller MA & Weissleder R Imaging of anticancer drug action in single cells. Nat. Rev. Cancer 17, 399–414 (2017). [PubMed: 28642603]
32. Coste A, Oktay MH, Condeelis JS & Entenberg D Intravital imaging techniques for biomedical and clinical research. Cytom. A 97, 448–457 (2020).
33. Cahalan MD, Parker I, Wei SH & Miller MJ Real-time imaging of lymphocytes in vivo. Curr. Opin. Immunol 15, 372–377 (2003). [PubMed: 12900266]
34. Zinselmeyer BH, Lynch JN, Zhang X, Aoshi T & Miller MJ Video-rate two-photon imaging of mouse footpad - a promising model for studying leukocyte recruitment dynamics during inflammation. Inflamm. Res 57, 93–96 (2008). [PubMed: 18213448]
35. You S et al. Intravital imaging by simultaneous label-free autofluorescence-multiharmonic microscopy. Nat. Commun 9, 2125 (2018). [PubMed: 29844371]
36. Wang T et al. Three-photon imaging of mouse brain structure and function through the intact skull. Nat. Methods 15, 789–792 (2018). [PubMed: 30202059]
37. Mahou P et al. Multicolor two-photon tissue imaging by wavelength mixing. Nat. Methods 9, 815–818 (2012). [PubMed: 22772730]
38. Provenzano PP, Eliceiri KW & Keely PJ Multiphoton microscopy and fluorescence lifetime imaging microscopy (FLIM) to monitor metastasis and the tumor microenvironment. Clin. Exp. Metastasis 26, 357–370 (2009). [PubMed: 18766302]
39. Wang Y et al. Direct visualization of the phenotype of hypoxic tumor cells at single cell resolution in vivo using a new hypoxia probe. Intravital 5, e1187803 (2016). [PubMed: 27790387]
40. Aguirre-Ghiso JA, Ossowski L & Rosenbaum SK Green fluorescent protein tagging of extracellular signal-regulated kinase and p38 pathways reveals novel dynamics of pathway activation during primary and metastatic growth. Cancer Res. 64, 7336–7345 (2004). [PubMed: 15492254]
41. Sharma VP et al. Live tumor imaging shows macrophage induction and TMEM-mediated enrichment of cancer stem cells during metastatic dissemination. Nat. Commun 12, 7300 (2021). [PubMed: 34911937] This work uses high-resolution intravital microscopy of a fluorescent biosensor for CSCs to discover that tumour-associated macrophages induce a stem-like phenotype in migrating breast cancer cells as the tumour cells enter the vasculature.
42. Dorand RD, Barkauskas DS, Evans TA, Petrosiute A & Huang AY Comparison of intravital thinned skull and cranial window approaches to study CNS immunobiology in the mouse cortex. Intravital 10.4161/intv.29728 (2014).
43. Cabrera M & Frevert U Novel in vivo imaging techniques for the liver microvasculature. Intravital 1, 107–114 (2012).
44. Ritsma L et al. Surgical implantation of an abdominal imaging window for intravital microscopy. Nat. Protoc 8, 583–594 (2013). [PubMed: 23429719]
45. Siemionow M & Nanhekhan LV Introduction of cremaster muscle chamber technique for long-term intravital microscopy. Ann. Plast. Surg 43, 161–166 (1999). [PubMed: 10454323]
46. Kawakami N Intravital imaging of T cells within the spinal cord. Methods Mol. Biol 1763, 119–127 (2018). [PubMed: 29476493]
47. Fenrich KK et al. Long-term in vivo imaging of normal and pathological mouse spinal cord with subcellular resolution using implanted glass windows. J. Physiol 590, 3665–3675 (2012). [PubMed: 22641787]

48. Entenberg D et al. Time-lapsed, large-volume, high-resolution intravital imaging for tissue-wide analysis of single cell dynamics. Methods 128, 65–77 (2017). [PubMed: 28911733] This article provides techniques for achieving LVHR-IVI in a variety of tissues, and describes how this LVHR-IVI can yield multiscale images that provide information similar to that obtained by pathologists when analysing fixed tissues.
49. Williams JK et al. Validation of a device for the active manipulation of the tumor microenvironment during intravital imaging. Intravital 5, e1182271 (2016). [PubMed: 27790386]
50. Bochner F, Fellus-Alyagor L, Kalchenko V, Shinar S & Neeman M A novel intravital imaging window for longitudinal microscopy of the mouse ovary. Sci. Rep 5, 12446 (2015). [PubMed: 26207832]
51. Dunn KW, Sutton TA & Sandoval RM Live-animal imaging of renal function by multiphoton microscopy. Curr. Protoc. Cytom 10.1002/0471142956.cy1209s41 (2007).
52. Das S et al. Tumor cell entry into the lymph node is controlled by CCL1 chemokine expressed by lymph node lymphatic sinuses. J. Exp. Med 210, 1509–1528 (2013). [PubMed: 23878309]
53. Zolla V et al. Aging-related anatomical and biochemical changes in lymphatic collectors impair lymph transport, fluid homeostasis, and pathogen clearance. Aging Cell 14, 582–594 (2015). [PubMed: 25982749]
54. Sellers SL & Payne GW Intravital microscopy of the inguinal lymph node. J. Vis. Exp 10.3791/2551 (2011).
55. Meijer EFJ et al. Murine chronic lymph node window for longitudinal intravital lymph node imaging. Nat. Protoc 12, 1513–1520 (2017). [PubMed: 28683064]
56. Masedunskas A, Porat-Shliom N, Tora M, Milberg O & Weigert R Intravital microscopy for imaging subcellular structures in live mice expressing fluorescent proteins. J. Vis. Exp 10.3791/50558 (2013).
57. Entenberg D et al. In vivo subcellular resolution optical imaging in the lung reveals early metastatic proliferation and motility. Intravital 4, 1–11 (2015). [PubMed: 26855844]
58. Entenberg D et al. A permanent window for the murine lung enables high-resolution imaging of cancer metastasis. Nat. Methods 15, 73–80 (2018). [PubMed: 29176592]
59. Huang Q et al. Intravital imaging of mouse embryos. Science 368, 181–186 (2020). [PubMed: 32273467]
60. Kishikova L, Norris JM & Smith MD Engineering the future of surgery: the place of the surgical engineering faculty. Surgery 153, 135 (2013). [PubMed: 23232029]
61. Riskin DJ, Longaker MT, Gertner M & Krummel TM Innovation in surgery: a historical perspective. Ann. Surg 244, 686–693 (2006). [PubMed: 17060760]
62. Ritsma L et al. Intravital microscopy through an abdominal imaging window reveals a pre-micrometastasis stage during liver metastasis. Sci. Transl Med 4, 158ra145 (2012).
63. Reismann D et al. Longitudinal intravital imaging of the femoral bone marrow reveals plasticity within marrow vasculature. Nat. Commun 8, 2153 (2017). [PubMed: 29255233]
64. Harney AS et al. Real-time imaging reveals local, transient vascular permeability, and tumor cell intravasation stimulated by TIE2hi macrophage-derived VEGFA. Cancer Discov. 5, 932–943 (2015). [PubMed: 26269515] This work uses IVI to study primary breast tumours and finds that tumour cell intravasation occurs at sites of transient vascular opening, restricted to intravasation sites known as TMEM doorways, and that intravasation is dependent on TIE2^{hi} TMEM macrophages.
65. Kienast Y et al. Real-time imaging reveals the single steps of brain metastasis formation. Nat. Med 16, 116–122 (2010). [PubMed: 20023634]
66. Laughney AM et al. Single-cell pharmacokinetic imaging reveals a therapeutic strategy to overcome drug resistance to the microtubule inhibitor eribulin. Sci. Transl Med 6, 261ra152 (2014).
67. Arlauckas SP et al. In vivo imaging reveals a tumor-associated macrophage-mediated resistance pathway in anti-PD-1 therapy. Sci. Transl Med 10.1126/scitranslmed.aal3604 (2017).
68. Nakasone ES et al. Imaging tumor-stroma interactions during chemotherapy reveals contributions of the microenvironment to resistance. Cancer Cell 21, 488–503 (2012). [PubMed: 22516258] This article provides an excellent example of how intravital microscopy can be used to investigate

the dynamics of cancer cell death in response to therapy in the in vivo TME, revealing drug distribution, cell death, and tumour–stroma interactions and gaining insights into drug responses in vivo.

69. Karagiannis GS et al. Neoadjuvant chemotherapy induces breast cancer metastasis through a TMEM-mediated mechanism. Sci. Transl Med 10.1126/scitranslmed.aan0026 (2017). Using fixed tissue and IVI, this work looks at the effect of chemotherapy on TMEM doorway-mediated breast cancer cell dissemination and finds that chemotherapy increases dissemination by increasing the density and activity of TMEM doorways and increases MENA expression.
70. Price DL et al. High-resolution large-scale mosaic imaging using multiphoton microscopy to characterize transgenic mouse models of human neurological disorders. Neuroinformatics 4, 65–80 (2006). [PubMed: 16595859]
71. Rios AC et al. Intraclonal plasticity in mammary tumors revealed through large-scale single-cell resolution 3D imaging. Cancer Cell 35, 618–632 (2019). [PubMed: 30930118]
72. Carmeliet P & Jain RK Principles and mechanisms of vessel normalization for cancer and other angiogenic diseases. Nat. Rev. Drug Discov 10, 417–427 (2011). [PubMed: 21629292]
73. Pinder SE Ductal carcinoma in situ (DCIS): pathological features, differential diagnosis, prognostic factors and specimen evaluation. Mod. Pathol 23 (Suppl. 2), 8–13 (2010).
74. Dunphy MP, Entenberg D, Toledo-Crow R & Larson SM In vivo microcartography and subcellular imaging of tumor angiogenesis: a novel platform for translational angiogenesis research. Microvasc. Res 78, 51–56 (2009). [PubMed: 19362098]
75. Amornphimoltham P, Thompson J, Melis N & Weigert R Non-invasive intravital imaging of head and neck squamous cell carcinomas in live mice. Methods 128, 3–11 (2017). [PubMed: 28780320]
76. Harper KL et al. Mechanism of early dissemination and metastasis in $Her2^{+}$ mammary cancer. Nature 540, 589–612 (2016). This work demonstrates (in part using LVHR-IVI) that tumour cell dissemination occurs even during the early stages of tumour evolution (before any apparent primary tumour masses are detected), and identifies the mechanism regulating this spread.
77. Borriello L et al. Primary tumor associated macrophages activate programs of invasion and dormancy in disseminating tumor cells. Nat. Commun 13, 626 (2022). [PubMed: 35110548] This work uses IVI to look at the fate of individual disseminated breast cancer cells as they arrive at the lung, and finds that, within the primary site, tumour-associated macrophages induce dissemination and dormancy phenotypes within a subset of tumour cells as the tumour cells enter the vasculature.
78. Wood S Jr Pathogenesis of metastasis formation observed in vivo in the rabbit ear chamber. AMA Arch. Pathol 66, 550–568 (1958). [PubMed: 13582395]
79. Sandison JC A new method for the microscopic study of living growing tissues by the introduction of a transparent chamber in the rabbit's ear. Anat. Rec 28, 281–287 (1924).
80. Morris VL et al. Early interactions of cancer cells with the microvasculature in mouse liver and muscle during hematogenous metastasis: videomicroscopic analysis. Clin. Exp. Metastasis 11, 377–390 (1993). [PubMed: 8375113]
81. Koike Y, Hatori M & Kokubun S Skeletal muscle metastasis secondary to cancer-a report of seven cases. Ups. J. Med. Sci 110, 75–83 (2005). [PubMed: 15801688]
82. Crist SB & Ghajar CM When a house is not a home: a survey of antimetastatic niches and potential mechanisms of disseminated tumor cell suppression. Annu. Rev. Pathol 16, 409–432 (2021). [PubMed: 33276706]
83. Crist SB et al. Unchecked oxidative stress in skeletal muscle prevents outgrowth of disseminated tumour cells. Nat. Cell Biol 24, 538–553 (2022). [PubMed: 35411081]
84. Hayashi K et al. Real-time imaging of tumor-cell shedding and trafficking in lymphatic channels. Cancer Res. 67, 8223–8228 (2007). [PubMed: 17804736]
85. Brown M et al. Lymph node blood vessels provide exit routes for metastatic tumor cell dissemination in mice. Science 359, 1408–1411 (2018). [PubMed: 29567714]
86. Pereira ER et al. Lymph node metastases can invade local blood vessels, exit the node, and colonize distant organs in mice. Science 359, 1403–1407 (2018). [PubMed: 29567713]
87. Coste A et al. Hematogenous dissemination of breast cancer cells from lymph nodes is mediated by tumor microenvironment of metastasis doorways. Front. Oncol 10, 571100 (2020). [PubMed: 33194666]

88. Young J Malpighi's "De Pulmonibus". Proc. R. Soc. Med 23, 1–11 (1929). [PubMed: 19987199]
89. Hall HL A study of the pulmonary circulation by the trans-illumination method. Am. J. Physiol. Leg. Content 72, 446–457 (1925).
90. Terry RJ A thoracic window for observation of the lung in a living animal. Science 90, 43–44 (1939). [PubMed: 17798138]
91. Funakoshi N et al. A new model of lung metastasis for intravital studies. Microvasc. Res 59, 361–367 (2000). [PubMed: 10792967]
92. Hatakawa H et al. Blood flow does not correlate with the size of metastasis in our new intravital observation model of Lewis lung cancer. Microvasc. Res 64, 32–37 (2002). [PubMed: 12074628]
93. Headley MB et al. Visualization of immediate immune responses to pioneer metastatic cells in the lung. Nature 531, 513–517 (2016). [PubMed: 26982733]
94. Borriello L, Traub B, Coste A, Oktay MH & Entenberg D A permanent window for investigating cancer metastasis to the lung. J. Vis. Exp 10.3791/62761 (2021).
95. Dai J et al. Astrocytic laminin-211 drives disseminated breast tumor cell dormancy in brain. Nat. Cancer 3, 25–42 (2022). [PubMed: 35121993]
96. Stelzer KJ Epidemiology and prognosis of brain metastases. Surg. Neurol. Int 4, S192–S202 (2013). [PubMed: 23717790]
97. Bagge U, Skolnik G & Ericson LE The arrest of circulating tumor cells in the liver microcirculation. A vital fluorescence microscopic, electron microscopic and isotope study in the rat. J. Cancer Res. Clin. Oncol 105, 134–140 (1983). [PubMed: 6826636]
98. Scherbarth S & Orr FW Intravital videomicroscopic evidence for regulation of metastasis by the hepatic microvasculature: effects of interleukin-1alpha on metastasis and the location of B16F1 melanoma cell arrest. Cancer Res. 57, 4105–4110 (1997). [PubMed: 9307300]
99. Schluter K et al. Organ-specific metastatic tumor cell adhesion and extravasation of colon carcinoma cells with different metastatic potential. Am. J. Pathol 169, 1064–1073 (2006). [PubMed: 16936278]
100. Sipkins DA et al. In vivo imaging of specialized bone marrow endothelial microdomains for tumour engraftment. Nature 435, 969–973 (2005). [PubMed: 15959517]
101. DiPiro JT, Spruill W, Wade W, Blouin RA & Pruemer JM in Concepts in Clinical Pharmacokinetics 5th edn (American Society of Health-System Pharmacists, 2010).
102. Cho S & Yoon YR Understanding the pharmacokinetics of prodrug and metabolite. Transl Clin. Pharmacol 26, 1–5 (2018). [PubMed: 32055540]
103. Tuntland T et al. Implementation of pharmacokinetic and pharmacodynamic strategies in early research phases of drug discovery and development at Novartis Institute of Biomedical Research. Front. Pharmacol 5, 174 (2014). [PubMed: 25120485]
104. Matthews PM, Rabiner EA, Passchier J & Gunn RN Positron emission tomography molecular imaging for drug development. Br. J. Clin. Pharmacol 73, 175–186 (2012). [PubMed: 21838787]
105. Bousso P Diving into the mechanism of action of tumor immunotherapies with intravital imaging. Immunol. Rev 306, 218–223 (2022). [PubMed: 34713901]
106. Momiyama M et al. Subcellular real-time imaging of the efficacy of temozolomide on cancer cells in the brain of live mice. Anticancer Res. 33, 103–106 (2013). [PubMed: 23267133]
107. Rodell CB et al. TLR7/8-agonist-loaded nanoparticles promote the polarization of tumour-associated macrophages to enhance cancer immunotherapy. Nat. Biomed. Eng 2, 578–588 (2018). [PubMed: 31015631]
108. Miller MA et al. Modular nanoparticulate prodrug design enables efficient treatment of solid tumors using bioorthogonal activation. ACS Nano 12, 12814–12826 (2018). [PubMed: 30550257]
109. Canel M et al. Quantitative in vivo imaging of the effects of inhibiting integrin signaling via Src and FAK on cancer cell movement: effects on E-cadherin dynamics. Cancer Res. 70, 9413–9422 (2010). [PubMed: 21045155]
110. Miller MA et al. Radiation therapy primes tumors for nanotherapeutic delivery via macrophage-mediated vascular bursts. Sci. Transl Med 9, eaal0225 (2017). [PubMed: 28566423] This article demonstrates how IVI can lead to new therapeutic approaches, by showing how radiotherapy

causes tumour-associated macrophages to accumulate adjacent to microvasculature, and that they then ‘prime’ the TME for improved drug responses by eliciting dynamic bursts of extravasation, and subsequently enhance drug delivery and uptake in neighbouring tumour cells.

111. Vennin C, Herrmann D, Lucas MC & Timpson P Intravital imaging reveals new ancillary mechanisms co-opted by cancer cells to drive tumor progression. F1000Res 5, 892 (2016).
112. Beltman JB, Maree AF & de Boer RJ Analysing immune cell migration. Nat. Rev. Immunol 9, 789–798 (2009). [PubMed: 19834485]
113. Meijering E, Dzyubachyk O & Smal I Methods for cell and particle tracking. Methods Enzymol. 504, 183–200 (2012). [PubMed: 22264535]
114. Entenberg D et al. Setup and use of a two-laser multiphoton microscope for multichannel intravital fluorescence imaging. Nat. Protoc 6, 1500–1520 (2011). [PubMed: 21959234]
115. Dawson CA, Mueller SN, Lindeman GJ, Rios AC & Visvader JE Intravital microscopy of dynamic single-cell behavior in mouse mammary tissue. Nat. Protoc 16, 1907–1935 (2021). [PubMed: 33627843]
116. Bares AJ et al. Hyperspectral multiphoton microscopy for in vivo visualization of multiple, spectrally overlapped fluorescent labels. Optica 7, 1587–1601 (2020). [PubMed: 33928182]
117. Rakhymzhan A et al. Method for multiplexed dynamic intravital multiphoton imaging. Methods Mol. Biol 2350, 145–156 (2021). [PubMed: 34331284]
118. Miska J et al. Real-time immune cell interactions in target tissue during autoimmune-induced damage and graft tolerance. J. Exp. Med 211, 441–456 (2014). [PubMed: 24567447]
119. Chawda C, McMorrow R, Gaspar N, Zambito G & Mezzanotte L Monitoring immune cell function through optical imaging: a review highlighting transgenic mouse models. Mol. Imaging Biol 24, 250–263 (2022). [PubMed: 34735680]
120. Fumagalli A et al. Plasticity of Lgr5-negative cancer cells drives metastasis in colorectal cancer. Cell Stem Cell 26, 569–578 (2020). [PubMed: 32169167] This article demonstrates how new fluorescent biosensors can be combined with IVI to reveal the behaviour and dynamics of CSCs during metastatic dissemination, finding that, in colorectal cancer, stemness is temporarily downregulated during the process of dissemination and then reactivated after arrival at the secondary site of the liver.
121. Tang B et al. A flexible reporter system for direct observation and isolation of cancer stem cells. Stem Cell Rep. 4, 155–169 (2015).
122. Helmlinger G, Yuan F, Dellian M & Jain RK Interstitial pH and pO2 gradients in solid tumors in vivo: high-resolution measurements reveal a lack of correlation. Nat. Med 3, 177–182 (1997). [PubMed: 9018236]
123. Gligorijevic B, Bergman A & Condeelis J Multiparametric classification links tumor microenvironments with tumor cell phenotype. PLoS Biol. 12, e1001995 (2014). [PubMed: 25386698]
124. Barth ND et al. A fluorogenic cyclic peptide for imaging and quantification of drug-induced apoptosis. Nat. Commun 11, 4027 (2020). [PubMed: 32788676] This article provides an excellent example of the new probes being developed for IVI: a highly stable fluorogenic peptide that selectively stains apoptotic cells in vitro and in vivo and is validated in vivo for quantification and imaging of drug-induced apoptosis.
125. Barth ND et al. A bivalent activatable fluorescent probe for screening and intravitaL imaging of chemotherapy-induced cancer cell death. Angew. Chem. Int. Ed 10.1002/anie.202113020 (2021).
126. Campagnola P Second harmonic generation imaging microscopy: applications to diseases diagnostics. Anal. Chem 83, 3224–3231 (2011). [PubMed: 21446646]
127. Datta R, Heaster TM, Sharick JT, Gillette AA & Skala MC Fluorescence lifetime imaging microscopy: fundamentals and advances in instrumentation, analysis, and applications. J. Biomed. Opt 25, 1–43 (2020).
128. Hato T et al. Two-photon intravital fluorescence lifetime imaging of the kidney reveals cell-type specific metabolic signatures. J. Am. Soc. Nephrol 28, 2420–2430 (2017). [PubMed: 28250053]
129. Szulczewski JM et al. In vivo visualization of stromal macrophages via label-free FLIM-based metabolite imaging. Sci. Rep 6, 25086 (2016). [PubMed: 27220760]

130. Leben R et al. Phasor-based endogenous NAD(P)H fluorescence lifetime imaging unravels specific enzymatic activity of neutrophil granulocytes preceding NETosis. Int. J. Mol. Sci 10.3390/ijms19041018 (2018).

131. Conway JRW et al. Intravital imaging to monitor therapeutic response in moving hypoxic regions resistant to PI3K pathway targeting in pancreatic cancer. Cell Rep. 23, 3312–3326 (2018). [PubMed: 29898401]

132. Sun Y et al. Fluorescence lifetime imaging microscopy for brain tumor image-guided surgery. J. Biomed. Opt 15, 056022 (2010). [PubMed: 21054116]

133. Sun Y et al. Endoscopic fluorescence lifetime imaging for in vivo intraoperative diagnosis of oral carcinoma. Microsc. Microanal 19, 791–798 (2013). [PubMed: 23702007]

134. Chang YS, Jalgaonkar SP, Middleton JD & Hai T Stress-inducible gene Atf3 in the noncancer host cells contributes to chemotherapy-exacerbated breast cancer metastasis. Proc. Natl Acad. Sci. USA 114, E7159–E7168 (2017). [PubMed: 28784776]

135. Borriello L, Condeelis J, Entenberg D & Oktay MH Breast cancer cell re-dissemination from lung metastases — a mechanism for enhancing metastatic burden. J. Clin. Med 10.3390/jcm10112340 (2021).

136. Zhang W et al. The bone microenvironment invigorates metastatic seeds for further dissemination. Cell 184, 2471–2486 (2021). [PubMed: 33878291] This work uses several approaches to demonstrate that metastatic breast and prostate tumour cells can remigrate from the bone to tertiary locations and that this effect is driven by epigenetic reprogramming that confers stem cell-like properties on the cancer cells.

137. Cherdyntseva NV, Litviakov NV, Denisov EV, Gervas PA & Cherdyntsev ES Circulating tumor cells in breast cancer: functional heterogeneity, pathogenetic and clinical aspects. Exp. Oncol 39, 2–11 (2017). [PubMed: 28361862]

138. Guller U et al. Disseminated single tumor cells as detected by real-time quantitative polymerase chain reaction represent a prognostic factor in patients undergoing surgery for colorectal cancer. Ann. Surg 236, 768–775 (2002). [PubMed: 12454515]

139. Yang C et al. Prognostic value of pre- and post-operative circulating tumor cells detection in colorectal cancer patients treated with curative resection: a prospective cohort study based on ISET device. Cancer Manag. Res 10, 4135–4144 (2018). [PubMed: 30323669]

140. Xie ZB, Yao L, Jin C & Fu DL Circulating tumor cells in pancreatic cancer patients: efficacy in diagnosis and value in prognosis. Discov. Med 22, 121–128 (2016). [PubMed: 27755967]

141. Friedl P, Locker J, Sahai E & Segall JE Classifying collective cancer cell invasion. Nat. Cell Biol 14, 777–783 (2012). [PubMed: 22854810]

142. Enterline HT & Coman DR The ameboid motility of human and animal neoplastic cells. Cancer 3, 1033–1038 (1950). [PubMed: 14783750]

143. Leighton J, Kalla RL, Turner JM Jr & Fennell RH Jr Pathogenesis of tumor invasion. II. Aggregate replication. Cancer Res. 20, 575–586 (1960). [PubMed: 14415447]

144. Giampieri S et al. Localized and reversible TGFbeta signalling switches breast cancer cells from cohesive to single cell motility. Nat. Cell Biol 11, 1287–1296 (2009). [PubMed: 19838175]

145. Ilina O et al. Intravital microscopy of collective invasion plasticity in breast cancer. Dis. Model. Mech 10.1242/dmm.034330 (2018).

146. Alexander S, Koehl GE, Hirschberg M, Geissler EK & Friedl P Dynamic imaging of cancer growth and invasion: a modified skin-fold chamber model. Histochem. Cell Biol 130, 1147–1154 (2008). [PubMed: 18987875]

147. Lin EY et al. Progression to malignancy in the polyoma middle T oncoprotein mouse breast cancer model provides a reliable model for human diseases. Am. J. Pathol 163, 2113–2126 (2003). [PubMed: 14578209] This work performs a detailed histological analysis of mammary tumour progression in the polyomavirus middle T antigen (PyMT) mouse model of breast cancer and compares it with that observed in humans, noting the morphological similarities as well as the consistency in biomarker expression between the two, thereby demonstrating that the PyMT mouse model is an excellent one to understand the biology of tumour progression in humans.

148. Beerling E, Oosterom I, Voest E, Lolkema M & van Rheenen J Intravital characterization of tumor cell migration in pancreatic cancer. Intravital 5, e1261773 (2016). [PubMed: 28243522]

This article characterizes migratory cells in primary pancreatic tumours using intravital microscopy and finds that pancreatic tumour cells migrate with a mesenchymal morphology as single individual cells or as a stream of non-cohesive single motile cells.

149. Deryugina EI & Kiosses WB Intratumoral cancer cell intravasation can occur independent of invasion into the adjacent stroma. Cell Rep. 19, 601–616 (2017). [PubMed: 28423322] This work analyses the spatial location of intravasation using explanted tissues and finds that intravasation occurs almost exclusively within the tumour core, involves intratumoural vasculature and does not involve vasculotropic cancer cells invading tumour-adjacent stroma and migrating along tumour-converging blood vessels.
150. Rohan TE et al. Tumor microenvironment of metastasis and risk of distant metastasis of breast cancer. J. Natl Cancer Inst 10.1093/jnci/dju136 (2014).
151. Robinson BD et al. Tumor microenvironment of metastasis in human breast carcinoma: a potential prognostic marker linked to hematogenous dissemination. Clin. Cancer Res 15, 2433–2441 (2009). [PubMed: 19318480]
152. Ginter PS et al. Tumor microenvironment of metastasis (TMEM) doorways are restricted to the blood vessel endothelium in both primary breast cancers and their lymph node metastases. Cancers 11, 1507 (2019). [PubMed: 31597373]
153. Nguyen-Ngoc KV et al. ECM microenvironment regulates collective migration and local dissemination in normal and malignant mammary epithelium. Proc. Natl Acad. Sci. USA 109, E2595–E2604 (2012). [PubMed: 22923691]
154. Khalil AA et al. Collective invasion in ductal and lobular breast cancer associates with distant metastasis. Clin. Exp. Metastasis 34, 421–429 (2017). [PubMed: 28894989]
155. Lugli A et al. Recommendations for reporting tumor budding in colorectal cancer based on the International Tumor Budding Consensus Conference (ITBCC) 2016. Mod. Pathol 30, 1299–1311 (2017). [PubMed: 28548122]
156. Rogers AC et al. Systematic review and meta-analysis of the impact of tumour budding in colorectal cancer. Br. J. Cancer 115, 831–840 (2016). [PubMed: 27599041]
157. van Wyk HC, Roxburgh CS, Horgan PG, Foulis AF & McMillan DC The detection and role of lymphatic and blood vessel invasion in predicting survival in patients with node negative operable primary colorectal cancer. Crit. Rev. Oncol. Hematol 90, 77–90 (2014). [PubMed: 24332522]
158. Mohammed RA et al. Objective assessment of lymphatic and blood vascular invasion in lymph node-negative breast carcinoma: findings from a large case series with long-term follow-up. J. Pathol 223, 358–365 (2011). [PubMed: 21171081]
159. Liotta LA, Saidel MG & Kleinerman J The significance of hematogenous tumor cell clumps in the metastatic process. Cancer Res. 36, 889–894 (1976). [PubMed: 1253177]
160. Duda DG et al. Malignant cells facilitate lung metastasis by bringing their own soil. Proc. Natl Acad. Sci. USA 107, 21677–21682 (2010). [PubMed: 21098274]
161. Kats-Ugurlu G et al. Circulating tumour tissue fragments in patients with pulmonary metastasis of clear cell renal cell carcinoma. J. Pathol 219, 287–293 (2009). [PubMed: 19731255]
162. Aceto N et al. Circulating tumor cell clusters are oligoclonal precursors of breast cancer metastasis. Cell 158, 1110–1122 (2014). [PubMed: 25171411]
163. Liu X et al. Homophilic CD44 interactions mediate tumor cell aggregation and polyclonal metastasis in patient-derived breast cancer models. Cancer Discov. 9, 96–113 (2019). [PubMed: 30361447] This work uses IVI to look at the origin of breast cancer tumour cell clusters in the blood circulation and the lung, and finds that tumour cell clusters are formed by intravasation of single tumour cells, which then cluster in the blood circulation owing to a high tumour cell expression of the cell-surface adhesion molecule CD44.
164. Thapa R & Wilson GD The importance of CD44 as a stem cell biomarker and therapeutic target in cancer. Stem Cell Int. 2016, 2087204 (2016).
165. Gkountela S et al. Circulating tumor cell clustering shapes DNA methylation to enable metastasis seeding. Cell 176, 98–112 (2019). [PubMed: 30633912]
166. Roussos ET et al. Mena invasive ($Mena^{INV}$) promotes multicellular streaming motility and transendothelial migration in a mouse model of breast cancer. J. Cell Sci 124, 2120–2131 (2011). [PubMed: 21670198]

167. Linde N et al. Macrophages orchestrate breast cancer early dissemination and metastasis. Nat. Commun 9, 21 (2018). [PubMed: 29295986]
168. Wyckoff JB et al. Direct visualization of macrophage-assisted tumor cell intravasation in mammary tumors. Cancer Res. 67, 2649–2656 (2007). [PubMed: 17363585]
169. Arwert EN et al. A unidirectional transition from migratory to perivascular macrophage is required for tumor cell intravasation. Cell Rep. 23, 1239–1248 (2018). [PubMed: 29719241]
170. Stella GM, Kolling S, Benvenuti S & Bortolotto C Lung-seeking metastases. Cancers 11, 1010 (2019). [PubMed: 31330946]
171. Qian B et al. A distinct macrophage population mediates metastatic breast cancer cell extravasation, establishment and growth. PLoS ONE 4, e6562 (2009). [PubMed: 19668347]
172. Ferjancic S et al. VCAM-1 and VAP-1 recruit myeloid cells that promote pulmonary metastasis in mice. Blood 121, 3289–3297 (2013). [PubMed: 23407548]
173. Wyckoff J et al. A paracrine loop between tumor cells and macrophages is required for tumor cell migration in mammary tumors. Cancer Res. 64, 7022–7029 (2004). [PubMed: 15466195]
174. Karagiannis GS, Goswami S, Jones JG, Oktay MH & Condeelis JS Signatures of breast cancer metastasis at a glance. J. Cell Sci 129, 1751–1758 (2016). [PubMed: 27084578]
175. Goswami S et al. Identification of invasion specific splice variants of the cytoskeletal protein Mena present in mammary tumor cells during invasion in vivo. Clin. Exp. Metastasis 26, 153–159 (2009). [PubMed: 18985426]
176. Gertler F & Condeelis J Metastasis: tumor cells becoming MENAcing. Trends Cell Biol. 21, 81–90 (2011). [PubMed: 21071226]
177. Leung E et al. Blood vessel endothelium-directed tumor cell streaming in breast tumors requires the HGF/C-Met signaling pathway. Oncogene 36, 2680–2692 (2017). [PubMed: 27893712]
178. Hughes VS, Wiggins JM & Siemann DW Tumor oxygenation and cancer therapy-then and now. Br. J. Radiol 10.1259/bjr.20170955 (2018).
179. Agarwal S et al. Quantitative assessment of invasive mena isoforms ($Mena^{calc}$) as an independent prognostic marker in breast cancer. Breast Cancer Res. 14, R124 (2012). [PubMed: 22971274]
180. Forse CL et al. Menacalc, a quantitative method of metastasis assessment, as a prognostic marker for axillary node-negative breast cancer. BMC Cancer 15, 483 (2015). [PubMed: 26112005]
181. Sparano JA et al. A metastasis biomarker (MetaSite Breast Score) is associated with distant recurrence in hormone receptor-positive, HER2-negative early-stage breast cancer. NPJ Breast Cancer 3, 42 (2017). [PubMed: 29138761]
182. Padera TP et al. Lymphatic metastasis in the absence of functional intratumor lymphatics. Science 296, 1883–1886 (2002). [PubMed: 11976409]
183. Pignatelli J et al. Macrophage-dependent tumor cell transendothelial migration is mediated by Notch1/$Mena^{INV}$-initiated invadopodium formation. Sci. Rep 6, 37874 (2016). [PubMed: 27901093]
184. Brown D et al. Phylogenetic analysis of metastatic progression in breast cancer using somatic mutations and copy number aberrations. Nat. Commun 8, 14944 (2017). [PubMed: 28429735]
185. Gundem G et al. The evolutionary history of lethal metastatic prostate cancer. Nature 520, 353–357 (2015). [PubMed: 25830880]
186. Harney AS et al. The selective Tie2 inhibitor rebastinib blocks recruitment and function of Tie2(Hi) macrophages in breast cancer and pancreatic neuroendocrine tumors. Mol. Cancer Ther 16, 2486–2501 (2017). [PubMed: 28838996]
187. Anampa Mesias JDS, Oktay MH, Xue X, Condeelis J & Sparano JA Phase Ib study of rebastinib plus antitubulin therapy with paclitaxel or eribulin in patients with metastatic breast cancer (MBC). J. Clin. Oncol 35 (Suppl. 15), TPS2611 (2017).
188. US National Library of Medicine. ClinicalTrials.gov and https://clinicaltrials.gov/ct2/show/NCT03717415 (2018).
189. US National Library of Medicine. ClinicalTrials.gov and https://clinicaltrials.gov/ct2/show/NCT02824575 (2016).
190. Gustavson M, Davis W, Bronsther O & Gertler F $Mena^{calc}$ as an independent prognostic factor and predictor of metastasis in non-small cell lung cancer. Cancer Res. 75, 4331–4331 (2015).

191. Naqvi I et al. Polymer-mediated inhibition of pro-invasive nucleic acid DAMPs and microvesicles limits pancreatic cancer metastasis. Mol. Ther 26, 1020–1031 (2018). [PubMed: 29550075]
192. Shaked Y The pro-tumorigenic host response to cancer therapies. Nat. Rev. Cancer 19, 667–685 (2019). [PubMed: 31645711]
193. Yuan F et al. Microvascular permeability and interstitial penetration of sterically stabilized (stealth) liposomes in a human tumor xenograft. Cancer Res. 54, 3352–3356 (1994). [PubMed: 8012948]
194. Yuan F et al. Vascular permeability and microcirculation of gliomas and mammary carcinomas transplanted in rat and mouse cranial windows. Cancer Res. 54, 4564–4568 (1994). [PubMed: 8062241]
195. Jain RK Normalizing tumor microenvironment to treat cancer: bench to bedside to biomarkers. J. Clin. Oncol 31, 2205–2218 (2013). [PubMed: 23669226]
196. Iyer AK, Khaled G, Fang J & Maeda H Exploiting the enhanced permeability and retention effect for tumor targeting. Drug. Discov. Today 11, 812–818 (2006). [PubMed: 16935749]
197. Fang J, Nakamura H & Maeda H The EPR effect: unique features of tumor blood vessels for drug delivery, factors involved, and limitations and augmentation of the effect. Adv. Drug Deliv. Rev 63, 136–151 (2011). [PubMed: 20441782]
198. Durfee PN et al. Mesoporous silica nanoparticle-supported lipid bilayers (protocells) for active targeting and delivery to individual leukemia cells. ACS Nano 10, 8325–8345 (2016). [PubMed: 27419663]
199. Ho YJ, Chang YC & Yeh CK Improving nanoparticle penetration in tumors by vascular disruption with acoustic droplet vaporization. Theranostics 6, 392–403 (2016). [PubMed: 26909113]
200. Boyerinas B et al. Adhesion to osteopontin in the bone marrow niche regulates lymphoblastic leukemia cell dormancy. Blood 121, 4821–4831 (2013). [PubMed: 23589674] This work uses IVI to demonstrate that blocking bone marrow niche signals can release leukaemic cells from dormancy, rendering these cells chemosensitive, and subsequently leading to a decrease in minimal residual disease.
201. Hirata E et al. Intravital imaging reveals how BRAF inhibition generates drug-tolerant microenvironments with high integrin beta1/FAK signaling. Cancer Cell 27, 574–588 (2015). [PubMed: 25873177] This work uses IVI to show that targeted therapy can indirectly activate melanoma cell proliferation pathways by stimulating non-cancerous cells within the TME, thereby rendering the targeted therapy ineffective.
202. Duarte D et al. Defining the in vivo characteristics of acute myeloid leukemia cells behavior by intravital imaging. Immunol. Cell Biol 97, 229–235 (2019). [PubMed: 30422351] By visualizing motility patterns of leukaemic cells with IVI, this work demonstrates that some leukaemias may respond poorly to chemotherapy owing to differences in bone marrow signals that allow the leukaemic cells to remain within the protective bone marrow niche.
203. Hawkins ED et al. T-cell acute leukaemia exhibits dynamic interactions with bone marrow microenvironments. Nature 538, 518–522 (2016). [PubMed: 27750279] This work uses IVI to observe stochastic interactions between leukaemic cells and the bone marrow niche and remodelling of the endosteal space by leukaemic cells, which indicates that novel therapies aimed at targeting these interactions may be beneficial in combating therapy-resistant disease.
204. Dings RP et al. Enhancement of T-cell-mediated antitumor response: angiostatic adjuvant to immunotherapy against cancer. Clin. Cancer Res 17, 3134–3145 (2011). [PubMed: 21252159] Using multiple approaches, including IVI, this work demonstrates that anti-angiogenic therapy, via altering the expression of receptors on endothelial cells to which leukocytes bind, may increase extravasation of leukocytes into the melanoma TME and thus increase the antitumour immune response.
205. Tanaka K et al. In vivo real-time imaging of chemotherapy response on the liver metastatic tumor microenvironment using multiphoton microscopy. Oncol. Rep 28, 1822–1830 (2012). [PubMed: 22923070]
206. Shaked Y Balancing efficacy of and host immune responses to cancer therapy: the yin and yang effects. Nat. Rev. Clin. Oncol 13, 611–626 (2016). [PubMed: 27118493]

207. Katz OB & Shaked Y Host effects contributing to cancer therapy resistance. Drug Resist. Updat 19, 33–42 (2015). [PubMed: 25575621]

208. Karagiannis GS, Condeelis JS & Oktay MH Chemotherapy-induced metastasis: mechanisms and translational opportunities. Clin. Exp. Metastasis 35, 269–284 (2018). [PubMed: 29307118]

209. Karagiannis GS, Condeelis JS & Oktay MH Chemotherapy-induced metastasis: molecular mechanisms, clinical manifestations, therapeutic interventions. Cancer Res. 79, 4567–4576 (2019). [PubMed: 31431464]

210. Okigami M et al. Intravital imaging of the effects of 5-fluorouracil on the murine liver microenvironment using 2-photon laser scanning microscopy. Oncol. Lett 11, 2433–2439 (2016). [PubMed: 27073493]

211. Wyckoff J, Gligorijevic B, Entenberg D, Segall J & Condeelis J High-resolution multiphoton imaging of tumors in vivo. Cold Spring Harb. Protoc 2011, 1167–1184 (2011). [PubMed: 21969629]

212. Centonze VE & White JG Multiphoton excitation provides optical sections from deeper within scattering specimens than confocal imaging. Biophys. J 75, 2015–2024 (1998). [PubMed: 9746543]

213. Vadakkan TJ, Culver JC, Gao L, Anhut T & Dickinson ME Peak multiphoton excitation of mCherry using an optical parametric oscillator (OPO). J. Fluoresc 19, 1103–1109 (2009). [PubMed: 19590939]

214. Makarov NS, Drobizhev M & Rebane A Two-photon absorption standards in the 550–1600 nm excitation wavelength range. Opt. Express 16, 4029–4047 (2008). [PubMed: 18542501]

215. Shcherbo D et al. Far-red fluorescent tags for protein imaging in living tissues. Biochem. J 418, 567–574 (2009). [PubMed: 19143658]

216. Piatkevich KD et al. Monomeric red fluorescent proteins with a large Stokes shift. Proc. Natl Acad. Sci. USA 107, 5369–5374 (2010). [PubMed: 20212155]

217. Kobat D et al. Deep tissue multiphoton microscopy using longer wavelength excitation. Opt. Express 17, 13354–13364 (2009). [PubMed: 19654740]

218. Sarder P et al. All-near-infrared multiphoton microscopy interrogates intact tissues at deeper imaging depths than conventional single- and two-photon near-infrared excitation microscopes. J. Biomed. Opt 18, 106012 (2013). [PubMed: 24150231]

219. Wang T & Xu C Three-photon neuronal imaging in deep mouse brain. Optica 7, 947–960 (2020).

220. Kong L & Cui M In vivo neuroimaging through the highly scattering tissue via iterative multi-photon adaptive compensation technique. Opt. Express 23, 6145–6150 (2015). [PubMed: 25836837]

221. Wang C et al. Multiplexed aberration measurement for deep tissue imaging in vivo. Nat. Methods 11, 1037–1040 (2014). [PubMed: 25128976]

222. Sinefeld D, Paudel HP, Ouzounov DG, Bifano TG & Xu C Adaptive optics in multiphoton microscopy: comparison of two, three and four photon fluorescence. Opt. Express 23, 31472–31483 (2015). [PubMed: 26698772]

223. Rodriguez C et al. An adaptive optics module for deep tissue multiphoton imaging in vivo. Nat. Methods 18, 1259–1264 (2021). [PubMed: 34608309]

224. Bakker GJ et al. Intravital deep-tumor single-beam 3-photon, 4-photon, and harmonic microscopy. Elife 10.7554/eLife.63776 (2022).

225. Miller DR, Jarrett JW, Hassan AM & Dunn AK Deep tissue imaging with multiphoton fluorescence microscopy. Curr. Opin. Biomed. Eng 4, 32–39 (2017). [PubMed: 29335679]

226. Ritsma L, Vrisekoop N & van Rheenen J In vivo imaging and histochemistry are combined in the cryosection labelling and intravital microscopy technique. Nat. Commun 4, 2366 (2013). [PubMed: 23978961] This work develops a microscopy technique, cryosection labelling and intravital microscopy, capable of correlating IVI videos with cryosections such that the same cells can be localized in each modality.

227. Karreman MA et al. Correlating intravital multi-photon microscopy to 3D electron microscopy of invading tumor cells using anatomical reference points. PLoS ONE 9, e114448 (2014). [PubMed: 25479106]

228. Karreman MA et al. Fast and precise targeting of single tumor cells in vivo by multimodal correlative microscopy. J. Cell Sci 129, 444–456 (2016). [PubMed: 26659665] This work develops a microscopy technique capable of correlating IVI videos with electron microscopy by using X-ray computed tomography as an intermediate step to provide clearly identifiable structures in all modalities.

229. Hasin Y, Seldin M & Lusis A Multi-omics approaches to disease. Genome Biol. 18, 83 (2017). [PubMed: 28476144]

230. Karahalil B Overview of systems biology and omics technologies. Curr. Med. Chem 23, 4221–4230 (2016). [PubMed: 27686657]

231. Scupakova K et al. Cellular resolution in clinical MALDI mass spectrometry imaging: the latest advancements and current challenges. Clin. Chem. Lab. Med 58, 914–929 (2020). [PubMed: 31665113]

232. Wang N, Li X, Wang R & Ding Z Spatial transcriptomics and proteomics technologies for deconvoluting the tumor microenvironment. Biotechnol. J 16, e2100041 (2021). [PubMed: 34125481]

233. Akturk G, Sweeney R, Remark R, Merad M & Gnjatic S Multiplexed immunohistochemical consecutive staining on single slide (MICSSS): multiplexed chromogenic IHC assay for high-dimensional tissue analysis. Methods Mol. Biol 2055, 497–519 (2020). [PubMed: 31502167]

234. Pascual-Reguant A et al. Multiplexed histology analyses for the phenotypic and spatial characterization of human innate lymphoid cells. Nat. Commun 12, 1737 (2021). [PubMed: 33741932]

235. Deisseroth K et al. Next-generation optical technologies for illuminating genetically targeted brain circuits. J. Neurosci 26, 10380–10386 (2006). [PubMed: 17035522]

236. Zhang K & Cui B Optogenetic control of intracellular signaling pathways. Trends Biotechnol. 33, 92–100 (2015). [PubMed: 25529484]

237. Rost BR, Schneider-Warme F, Schmitz D & Hegemann P Optogenetic tools for subcellular applications in neuroscience. Neuron 96, 572–603 (2017). [PubMed: 29096074]

238. Manoilov KY, Verkhusha VV & Shcherbakova DM A guide to the optogenetic regulation of endogenous molecules. Nat. Methods 18, 1027–1037 (2021). [PubMed: 34446923]

239. Nagel G et al. Channelrhodopsin-2, a directly light-gated cation-selective membrane channel. Proc. Natl Acad. Sci. USA 100, 13940–13945 (2003). [PubMed: 14615590]

240. Mills E, Chen X, Pham E, Wong S & Truong K Engineering a photoactivated caspase-7 for rapid induction of apoptosis. ACS Synth. Biol 1, 75–82 (2012). [PubMed: 23651071]

241. Reichhart E, Ingles-Prieto A, Tichy AM, McKenzie C & Janovjak H A phytochrome sensory domain permits receptor activation by red light. Angew. Chem. Int. Ed 55, 6339–6342 (2016).

242. Buckley CE et al. Reversible optogenetic control of subcellular protein localization in a live vertebrate embryo. Dev. Cell 36, 117–126 (2016). [PubMed: 26766447]

243. Zhou XX, Chung HK, Lam AJ & Lin MZ Optical control of protein activity by fluorescent protein domains. Science 338, 810–814 (2012). [PubMed: 23139335]

244. Konermann S et al. Optical control of mammalian endogenous transcription and epigenetic states. Nature 500, 472–476 (2013). [PubMed: 23877069]

245. Pathak GP et al. Bidirectional approaches for optogenetic regulation of gene expression in mammalian cells using Arabidopsis cryptochrome 2. Nucleic Acids Res. 45, e167 (2017). [PubMed: 28431041]

246. Joshi J, Rubart M & Zhu W Optogenetics: background, methodological advances and potential applications for cardiovascular research and medicine. Front. Bioeng. Biotechnol 7, 466 (2019). [PubMed: 32064254]

247. Krueger D et al. Principles and applications of optogenetics in developmental biology. Development 10.1242/dev.175067 (2019).

248. Weber J & Rad R Engineering CRISPR mouse models of cancer. Curr. Opin. Genet. Dev 54, 88–96 (2019). [PubMed: 31078083]

249. Scott GJ & Gruzdev A Genome editing in mouse embryos with CRISPR/Cas9. Methods Mol. Biol 1960, 23–40 (2019). [PubMed: 30798518]

250. Chen Y et al. How is flexible electronics advancing neuroscience research. Biomaterials 268, 120559 (2021). [PubMed: 33310538]
251. Samineni VK et al. Fully implantable, battery-free wireless optoelectronic devices for spinal optogenetics. Pain 158, 2108–2116 (2017). [PubMed: 28700536]
252. Mondello SE et al. A micro-LED implant and technique for optogenetic stimulation of the rat spinal cord. Exp. Neurol 335, 113480 (2021). [PubMed: 32991934]
253. Keshmiri Neghab H et al. The state of the art of biomedical applications of optogenetics. Lasers Surg. Med 54, 202–216 (2022). [PubMed: 34363230]
254. Moghadam MR & Chen YP Tracking leukocytes in intravital time lapse images using 3D cell association learning network. Artif. Intell. Med 118, 102129 (2021). [PubMed: 34412846]
255. Khorshed RA et al. Automated identification and localization of hematopoietic stem cells in 3D intravital microscopy data. Stem Cell Rep. 5, 139–153 (2015).
256. Pizzagalli DU et al. Leukocyte tracking database, a collection of immune cell tracks from intravital 2-photon microscopy videos. Sci. Data 5, 180129 (2018). [PubMed: 30015806]
257. Pizzagalli DU et al. Characterization of the dynamic behavior of neutrophils following influenza vaccination. Front. Immunol 10, 2621 (2019). [PubMed: 31824481]
258. Shaner NC, Steinbach PA & Tsien RY A guide to choosing fluorescent proteins. Nat. Methods 2, 905–909 (2005). [PubMed: 16299475]
259. Shcherbakova DM, Stepanenko OV, Turoverov KK & Verkhusha VV Near-infrared fluorescent proteins: multiplexing and optogenetics across scales. Trends Biotechnol. 36, 1230–1243 (2018). [PubMed: 30041828]
260. Skala MC et al. In vivo multiphoton microscopy of NADH and FAD redox states, fluorescence lifetimes, and cellular morphology in precancerous epithelia. Proc. Natl Acad. Sci. USA 104, 19494–19499 (2007). [PubMed: 18042710]
261. Kedrin D et al. Intravital imaging of metastatic behavior through a mammary imaging window. Nat. Methods 5, 1019–1021 (2008). [PubMed: 18997781]
262. He HJ et al. Fluorescence resonance energy transfer-based method for detection of DNA binding activities of nuclear factor kappaB. Biotechniques 43, 93–98 (2007). [PubMed: 17695258]
263. Bravo-Cordero JJ, Moshfegh Y, Condeelis J & Hodgson L Live cell imaging of RhoGTPase biosensors in tumor cells. Methods Mol. Biol 1046, 359–370 (2013). [PubMed: 23868600]
264. Sakaue-Sawano A et al. Visualizing spatiotemporal dynamics of multicellular cell-cycle progression. Cell 132, 487–498 (2008). [PubMed: 18267078]
265. Keely P & Nain A Capturing relevant extracellular matrices for investigating cell migration. F1000Res 4, 1408 (2015).
266. Weigelin B, Bakker G-J & Friedl P Intravital third harmonic generation microscopy of collective melanoma cell invasion: principles of interface guidance and microvesicle dynamics. Intravital 1, 32–43 (2012). [PubMed: 29607252]
267. Shan S, Sorg B & Dewhirst MW A novel rodent mammary window of orthotopic breast cancer for intravital microscopy. Microvasc. Res 65, 109–117 (2003). [PubMed: 12686168]
268. Jeong HS et al. Investigation of the lack of angiogenesis in the formation of lymph node metastases. J. Natl Cancer Inst 107, djv155 (2015). [PubMed: 26063793]
269. Xu HT, Pan F, Yang G & Gan WB Choice of cranial window type for in vivo imaging affects dendritic spine turnover in the cortex. Nat. Neurosci 10, 549–551 (2007). [PubMed: 17417634]
270. Askoxylakis V et al. A cerebellar window for intravital imaging of normal and disease states in mice. Nat. Protoc 12, 2251–2262 (2017). [PubMed: 28981123]
271. Figley SA et al. A spinal cord window chamber model for in vivo longitudinal multimodal optical and acoustic imaging in a murine model. PLoS ONE 8, e58081 (2013). [PubMed: 23516432]
272. Fenrich KK, Weber P, Rougon G & Debarbieux F Long- and short-term intravital imaging reveals differential spatiotemporal recruitment and function of myelomonocytic cells after spinal cord injury. J. Physiol 591, 4895–4902 (2013). [PubMed: 23918770]
273. Black J Biological Performance of Materials: Fundamentals of Biocompatibility 4th edn (CRC Press, 2006).

274. Paik S et al. A multigene assay to predict recurrence of tamoxifen-treated, node-negative breast cancer. N. Engl. J. Med 351, 2817–2826 (2004). [PubMed: 15591335]

Box 1

New tools for intravital imaging

Encoded fluorescent proteins (CFP, GFP and YFP) and markers (fluorescent dextran and quantum dots)

Most commonly used markers for intravital imaging[258].

Near-infrared fluorescent probes

Allow increased multichannel imaging[259].

Fluorescence Lifetime Imaging

Used to image intrinsic fluorescence in unlabelled tissues[38,260].

Encoded photoconvertible fluorescent proteins (for example, Dendra2)

Used for fate mapping cells in living tissues at single-cell resolution[261].

Biosensors

Used for imaging of hypoxia[39], NF-κB[262], cancer stem cells[41,121], dormancy[40], Rho GTPases[263] and the cell cycle[264].

Second-harmonic generation

Used to image intrinsic nonlinear signal generation by extracellular matrix fibres[265].

Third-harmonic generation

Allows imaging of intrinsic nonlinear signal generation that relies on the light-scattering properties and mismatches of refractive indices of water–lipid and water–protein interfaces[266].

Box 2

Imaging windows for use with intravital imaging

Mammary

The mammary imaging window was developed to eliminate the limitations of the terminal skin flap and dorsal skin fold chamber techniques and allow serial visualization of the mammary gland and orthotopic mammary tumours at high resolution, and over a period spanning days to weeks[261,267].

Lymph node

The chronic inguinal lymph node window provides serial access to this important immunological tissue. This procedure is well tolerated without any significant physiological changes in the mouse 14 days after window implantation[268].

Abdominal

An abdominal window provides serial access to visceral organs, such as the spleen, kidneys, small intestine, pancreas and liver[62].

Lung

A permanent window for high-resolution imaging of the lung was developed to enable longitudinal imaging during cancer metastasis[58].

Cranial

Two different methods enable imaging access to the cortex of the mouse brain: the cranial imaging window and the thinned-skull cranial imaging window[269].

Cerebellum

The chronic cranial imaging window has been modified to image the mouse cerebellum, a region of the brain critical to coordinated motion[270].

Long bone

Longitudinal intravital imaging of the bone marrow allows long-term multiphoton imaging in the long bone using a gradient refractive index micro-endoscopic lens[63].

Ovarian

The ovarian imaging window is a long-term imaging window developed to study the maturation of the ovarian follicle in response to gonadotropin analogues, as well as tumour invasion into the ovary[50].

Spinal cord

Long-term imaging of the spinal cord can be accomplished for periods up to months[271,272].

Box 3

Imaging window designs and limitations

A list of imaging windows (and the tissues they give access to) in current use is given in Box 2. In designing new windows, attention must be paid to a fair number of parameters. Chief among these are shape and ergonomics to avoid irritation during ambulation, which leads to premature failure. Materials must be chosen with consideration given to biocompatibility, ease of manufacture and sterilizability. Biocompatibility must include evaluation of the impact of the material on the biology, as well as the biological impact on the material, as even materials normally considered inert (for example, ultra-high-molecular-weight polyethylene) can degrade over long periods of contact with tissues. Degraded materials can cause inflammation, allergic foreign-body responses or even chemical-induced carcinogenesis[273]. The importance of biocompatibility increases with the duration of implantation, but many chronic windows have been demonstrated to have exceptional performance over long periods[58,62,63].

For those not wishing to design their own custom windows, many publications include (and many laboratories are willing to share) manufacturing drawings that can be brought to in-house machine shops. If these services are not available, investigators can perform an Internet search for some of the nascent online custom manufacturing marketplaces where drawings can be uploaded to a website and machine shops with available capacity bid for the work.

Finally, optical performance must be evaluated, ensuring that the tissue is within the working distance of the objective lens, the point spread function of the illumination light is maintained and optical clarity is preserved over time. Use of standard no. 1.5 coverslip glass is usually sufficient to preserve point spread function, and some have reported that light-scattering proteinaceous deposits can be reduced or eliminated by coating coverslips with a polyethylene glycol film[44].

Box 4

Complementary use of the TMEM doorway score and the Oncotype DX Breast Recurrence Score in treatment decisions

The density of tumour microenvironment of metastasis (TMEM) doorways (TMEM doorway score) is an independent prognosticator of metastasis in breast cancer[150,151,181]. The TMEM doorway score offers the opportunity to fine-tune breast cancer prognosis obtained by the Oncotype DX Breast Recurrence Score (RS). RS is a 21-gene prognostic assay of recurrence based on genes predominantly associated with cancer cell proliferation[274]. In breast cancers from patients, there is a lack of correlation between these scores[181], indicating that they measure different aspects of cancer biology: the TMEM doorway score is a measure of cancer cell dissemination, while RS is a measure of cancer cell proliferation[174]. Indeed, patients with a low RS but a high TMEM doorway score have significantly increased risk of distant recurrence[174,181]. Thus, precision medicine should strive for the optimal assessment of prognosis by taking into consideration both scores when patient prognosis is being assessed and treatment is being planned.

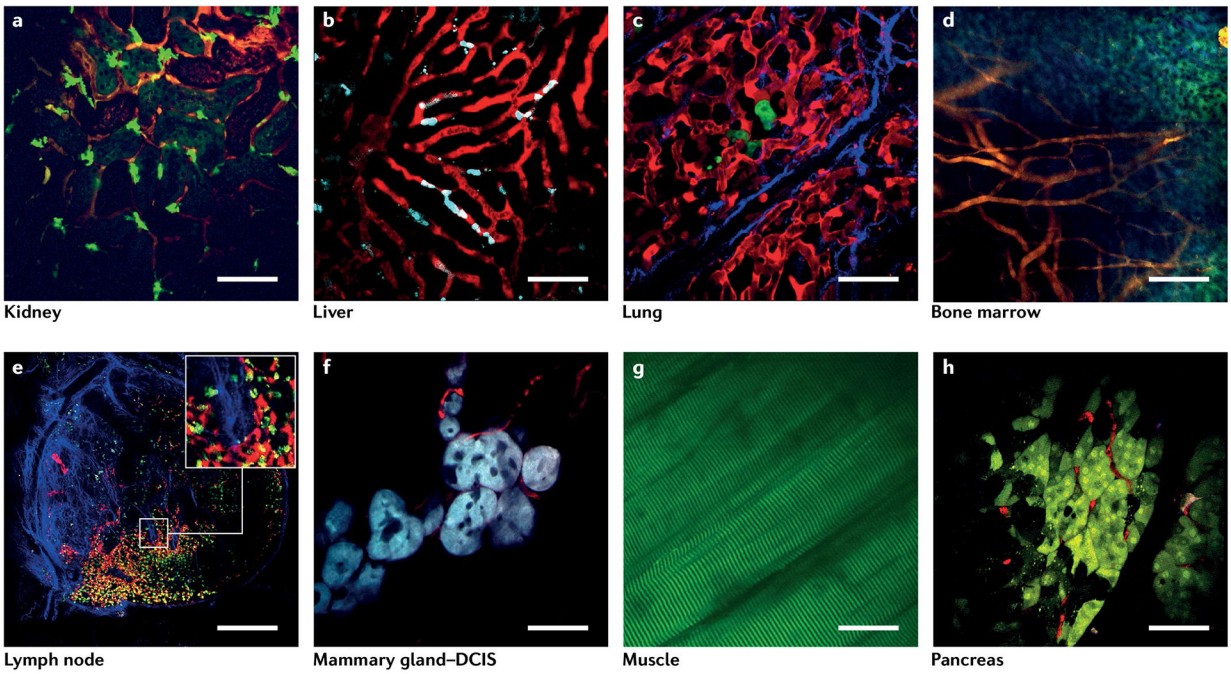

Fig. 1 |. Example images obtained by intravital imaging taken from a variety of tissues.
a, Kidney. Red, vasculature labelled with an Intravenous (IV) injection of tetramethylrhodamine (TMR)-tagged 155-kDa dextran; bright green, GFP-labelled macrophages; dim green, autofluorescence from collecting ducts and tubules. Scale bar, 70 μm. **b**, Liver. Red, sinusoids labelled with TMR-tagged 155-kDa dextran; cyan, CFP-labelled Kupffer cells. Scale bar, 70 μm. **c**, Lung. Red, vasculature labelled with an IV injection of TMR-tagged 155-kDa dextran; green, GFP-labelled disseminated tumour cells; blue, second-harmonic generation signal from type I collagen fibres. Scale bar, 70 μm. **d**, Bone marrow: a 3 × 3 mosaic of bone marrow imaged through the calvarium. Orange, vasculature labelled with an IV injection of TMR-tagged 155-kDa dextran; blue and green, autofluorescence from bone. Scale bar, 170 μm. **e**, Lymph node: a 5 × 5 mosaic of the entire lymph node. Red, blood vasculature labelled with an IV injection of TMR-tagged 155-kDa dextran and lymphatic endothelia ($PROX1^+$ cells) labelled with tdTomato; green, GFP-labelled macrophages; yellow, GFP-labelled macrophages that have taken up the TMR-tagged dextran; blue, second-harmonic generation signal from type I collagen fibres. Scale bar, 225 μm. The inset shows a zoomed view of the region in the white box. **f**, Ductal carcinoma in situ (DCIS) in the mammary gland. Cyan, CFP-labelled mammary epithelium at the DCIS stage; red, vasculature labelled with an IV injection of TMR-tagged 155-kDa dextran. Scale bar, 50 μm. **g**, Muscle. Green, autofluorescence from striated muscle fibres. Scale bar, 100 μm. **h**, Pancreas. Green, Dendra2-labelled pancreatic acinar cells; red, vasculature labelled with an IV injection of TMR-tagged 155-kDa dextran. Scale bar, 70 μm.

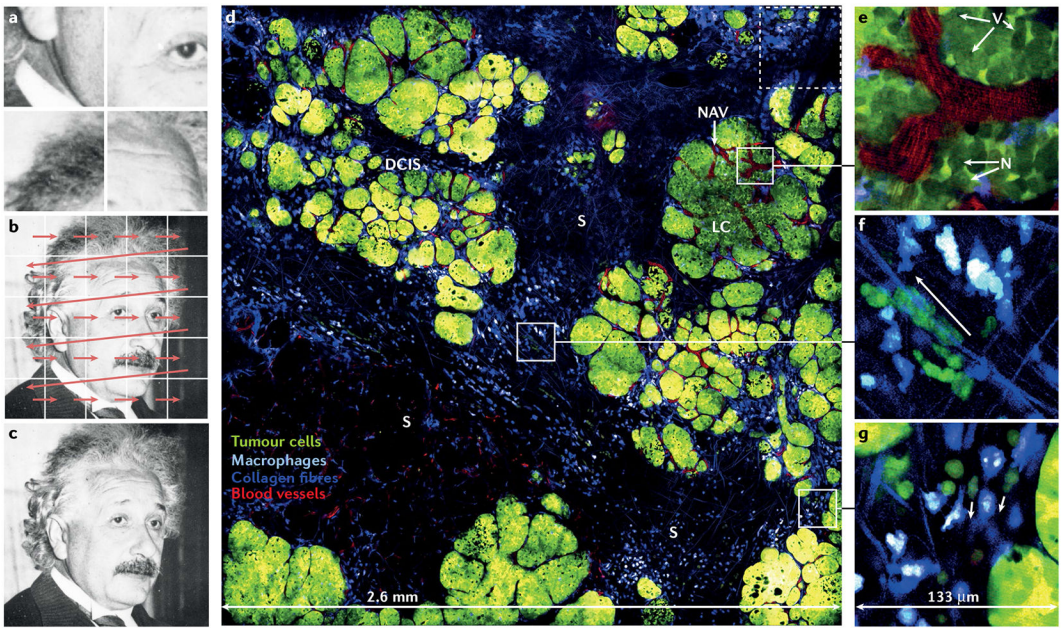

Fig. 2 |. Large-volume, high-resolution intravital imaging.

a, When presented with just a few high-resolution, high-magnification images, it is impossible to determine the subject of the photograph. **b**, Acquiring many images in a mosaicked pattern (orange arrows) maintains the spatial relationship between the individual acquired images. **c**, This allows complete coverage of the subject, and enables stitching of the individual images into a low-magnification, high-resolution image revealing the overall large-scale image. **d**, Large-volume, high-resolution intravital imaging (LVHR-IVI) applied to a mammary tumour using the method described previously[48] in a mouse mammary tumour virus–polyomavirus middle T antigen (MMTV-PyMT)–Dendra2 MacBlue mouse provides the context required to identify neoangiogenic vessels (NAVs) labelled with fluorescently tagged dextran (red) injected intravenously, distinguish between areas of ductal carcinoma in situ (DCIS) and late-stage carcinoma (LC), and determine their positioning relative to the stroma (S). A10 × 10 mosaic (340 μm × 340 μm tiles; the dashed box indicates the size of one tile) was acquired with a low-magnification, high-numerical aperture (NA) objective lens (25 × 1.05 NA). Fields of view were overlapped to compensate for non-uniform flatness of field illumination. Stitched images show the overall structure of the tissue. The formation of the ductal tree by the epithelial cells (green) is clearly visible, as are the blood vessels. **e**–**g**, The individual high-resolution tiles within the low-magnification LVHR-IVI image demonstrate the level of cellular and subcellular detail captured by this technique. **e**, Nuclei (N) and vacuoles (V). **f**, Cancer cell streaming migration along collagen fibres (arrow). **g**, Single-cell migration (arrows). Blue, second-harmonic generation signal from collagen I fibres; cyan, CFP-labelled macrophages; green, Dendra2-labelled tumour cells; red, tetramethylrhodamine-labelled 155-kDa dextran. The photograph in part **c** (and variations of it in parts **a**,**b**) courtesy of Keystone/Stringer via Getty Images.

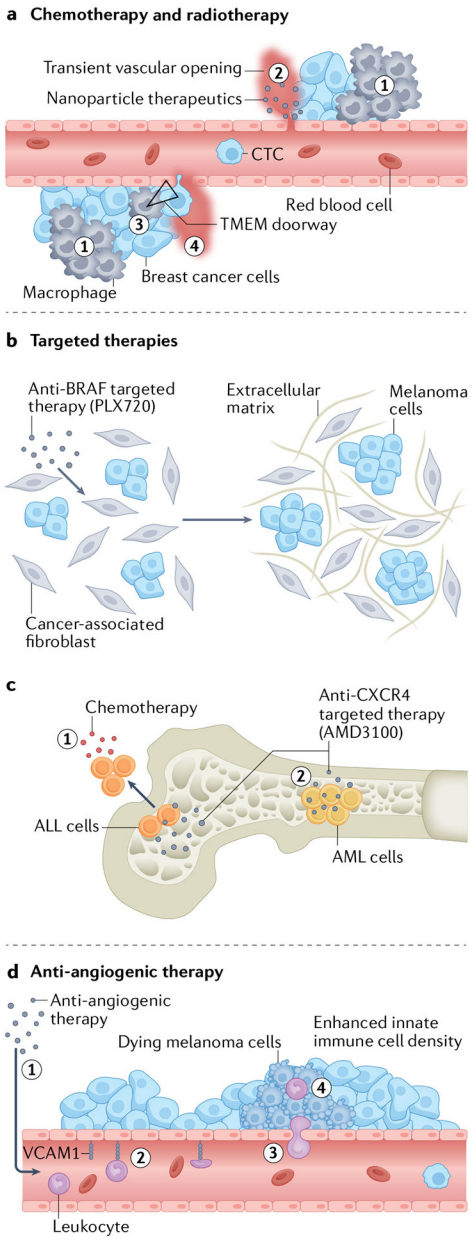

Fig. 3 |. The contribution of high-resolution intravital imaging to our understanding of the effects of various therapies on the tumour microenvironment and cancer phenotype.

a, Chemotherapy-and radiotherapy-induced tissue damage and hypoxia lead to an influx of myeloid cells (1) into the tumour microenvironment (TME)[68] and a subsequent increase in macrophage-mediated localized transient vascular openings that may affect drug delivery (2)[110] and may increase the density and activity of TME of metastasis (TMEM) doorways (triangle) (3), leading to enhanced localized TMEM doorway-mediated transient vascular opening (4), TMEM doorway-mediated single cancer cell intravasation and an increase in the number of circulating tumour cells (CTCs)[69]. **b**, Targeted therapy (for example, anti-BRAF) can lead to extracellular matrix remodelling via cells of the TME such as cancer-associated fibroblasts. The newly formed extracellular matrix may, by an alternative route,

activate growth signalling pathways, thereby bypassing the inhibited pathway and rendering the targeted therapy ineffective[201]. **c**, Targeted inhibition of C-X-C motif chemokine receptor 4 (CXCR4) prevents interaction of acute lymphoblastic leukaemia (ALL) cells with the bone marrow niche, allowing them to escape the bone marrow and become sensitive to chemotherapy (1). By contrast, other factors within the niche keep acute myeloid leukaemia (AML) cells within the marrow (2), rendering them insensitive to chemotherapy[202,203]. **d**, Anti-angiogenic therapy (1) can induce expression of endothelial adhesion molecules (for example, intercellular adhesion molecule 1 (ICAM1) and vascular cell adhesion molecule 1 (VCAM1)), which enhances leukocyte adhesion (2), leukocyte extravasation (3) and a subsequent antitumour immune response (4)[204].